

MAR 23 1964



Technical Note

No. 210

**AN ATLAS OF SOLAR FLARE EFFECTS
OBSERVED ON LONG VLF PATHS
DURING 1961**

C. J. CHILTON, F. K. STEELE, AND D. D. CROMBIE



U. S. DEPARTMENT OF COMMERCE
NATIONAL BUREAU OF STANDARDS

NATIONAL BUREAU OF STANDARDS

Technical Note 210

Issued March 13, 1964

AN ATLAS OF SOLAR FLARE EFFECTS OBSERVED ON LONG VLF PATHS DURING 1961

C. J. Chilton, F. K. Steele, and D. D. Crombie

Central Radio Propagation Laboratory

National Bureau of Standards

Boulder, Colorado

NBS Technical Notes are designed to supplement the Bureau's regular publications program. They provide a means for making available scientific data that are of transient or limited interest. Technical Notes may be listed or referred to in the open literature.

For sale by the Superintendent of Documents, U. S. Government Printing Office
Washington, D.C. 20402

Price 30¢

CONTENTS

	Page
Abstract	1
1. Introduction	1
2. Experimental Observations and Description of the Data . .	2
3. Acknowledgments	4
4. References	4
Figures	5
Tables	30

AN ATLAS OF SOLAR FLARE EFFECTS OBSERVED ON LONG
VLF PATHS DURING 1961

C. J. Chilton, F. K. Steele, and D. D. Crombie

Effects produced by 37 solar flares
on four long VLF paths during 1961 are
shown and tabulated.

1. Introduction

Since early in 1961, the phase and amplitude of various very-low-frequency transmissions have been monitored by the Boulder Laboratories of the National Bureau of Standards; the NBS field site at Maui, Hawaii; the Battelle Research Institute, Frankfurt, Germany; and the Geophysical Institute, College, Alaska. Observations of three phase-stabilized VLF transmissions over four long propagation paths were made at the above receiving sites using the VLF signals radiated from NBA(18 kc/s), Balboa, Panama; NPG(18.6 kc/s), Seattle, Washington; and GBR(16 kc/s), Rugby, England. The propagation paths, their respective lengths and geographic orientations are shown in figure 1. This VLF transmission network samples the variations occurring over approximately one quarter of the earth's surface and thus provides an excellent means for studying the effects of solar flare produced ionization over a large area of the ionosphere [Chilton, et al., 1963], as well as the normal day-to-night variation in ionospheric height.

Of the known perturbations which are observed in the recorded phase of a VLF transmission, the most easily recognizable are the Sudden Phase Anomalies (SPA's) [Bracewell and Straker, 1949], which are known to be produced by ionizing radiations emitted from the sun's chromosphere. These chromospheric flares, usually referred to as solar flares, are short-lived sudden increases in light intensity generally observed near sunspots. Optical observations show that almost all flares follow the same pattern, a rapid rise to peak intensity followed by a short period of peak intensity and a slow return to the pre-flare conditions. Typical flares have an onset time that varies from 1 to 30 minutes and the return to normal requires about 30 minutes to 2 or 3 hours. In order to provide a measure of their relative magnitude, flares have been divided into classes of importance (1, 2, 3 and 3+) according to their area and brightness. The surface area of Class 1 flares is on the order of 10^{-4} of the solar hemisphere, corresponding to a diameter of about 10^9 cm. The brightness factor is obtained by photometrically observing the H α line of the solar spectrum. The magnitude of the associated phase advance is apparently closely related to the increase in solar radiation, its energy spectrum, its angle of incidence at the lower regions of the ionosphere, and to the length of path over which a lowering of the apparent height of reflection occurs.

It is the sole purpose of this note to provide examples of the solar flare effects observed on the paths listed above during 1961. Emphasis has been placed on those flares for which observations are available on more than one path.

2. Experimental Observations and Description of the Data

The propagation paths are shown in figure 1. All of the paths except one (NPG-College) are sufficiently long to make it reasonable to assume that only one waveguide mode [Wait, 1962] is present. The data obtained with signals propagating along these paths show that during a solar flare the signals received over the sunlit paths exhibit sudden phase anomalies, which are not identical, either in magnitude or duration. These observations are illustrated in figures 2 through 25. These illustrations are photographic copies of the original records obtained between May 1 and December 2, 1961. In each case the phase and amplitude traces and the directions of phase advance and amplitude increase are identified. The records shown were chosen after examining all of the recorded data. Subsequently optical observations of solar flares as listed in the CRPL Series F, Part B (Solar-Geophysical Data) Bulletins were examined and times of optical sightings were obtained and added to the figures. In addition, the Solar-Geophysical Data were examined independently and times of all Class 1 or greater flares were obtained. The VLF data were then re-examined for solar flare effects at these times. Flares for which observations on two or more paths were available are included in figures 2-25, although some other flares are included because of their proximity in time to flares for which there are two or more observations. These figures contain effects observed during 37 flares. Included in the figures are some records for which there was no visual sighting; these records are very similar to those which are associated with flares and have been included for this reason. Also included are several records for which all the paths are not totally sunlit, but which nevertheless show an appreciable effect.

The SPA's and optical classification of the associated solar flares have been listed in chronological order in table 1, which in addition contains some of the more important characteristics of the SPA's, as scaled from the figures. Following the date, the optical class and time of optical sighting are listed. The next three columns list the time of first appearance of an effect on the phase records, the time of maximum effect, and the time of return to normal. Then the size of the phase anomaly $\Delta\phi$ in degrees, and in microseconds (Δt) is listed. The latter quantity, Δt is obtained from the relation

$$\Delta t = \frac{\Delta\phi}{0.36} \cdot \frac{1}{f}$$

where f is in kc/s. The size of the phase change $\Delta\phi$ produced by a given depression Δh of the ionosphere is not particularly useful in itself since it depends on the path length and the frequency of the signal, as well as on Δh . Thus Δh is a better index of the magnitude of the solar flare effect. So in the next column, values of Δh calculated in the manner described by Wait [1959, 1961] are given for all paths except NPG - College which, as noted above, is too short to assume that only one waveguide mode is present. These values of Δh are obtained on the assumption that the flare produces a constant depression along the whole path. This of course is hardly likely, since it would be reasonable to assume that the flare would produce the greatest effects at the sub-solar point, the effects becoming smaller as the zenith angle of sun increases. This might be corrected by relating the zenith angle (χ) to the calculated value of Δh since it has been shown [Chilton, et al., 1963] that when the observed Δh obtained on the above basis is plotted semilogarithmically against $1/\overline{\text{Cos } \chi}$, (where $\overline{\text{Cos } \chi}$ is the average value of $\text{Cos } \chi$ along the propagation path), a straight line results. Thus the table contains values of average χ and average $\text{Cos } \chi$ which are listed in the last two columns.

Table 1 also contains estimates of the maximum change of ϕ and ($d\phi/dt$) observed on each path, for each flare. Observed values of $d\phi/dt$ vary from as much as $90^\circ/\text{min}$ to as little as $1^\circ/\text{min}$.

In view of the wide geographical distribution of the paths on which these observations have been made, and of the distribution in time of occurrences of the flares, it seems reasonable to regard these observations as a sample of typical flare observations which might be made on any path at any time. Therefore, the scaled data from table 1 have been separated according to the optical classification of the originating flare. Table 2 thus contains for each flare of Class 1, 2 or 3, the maximum, mean, and minimum phase shifts, together with the phase shifts exceeded by 25%, 50%, and 75% of the observations. Similarly, table 3 contains corresponding values of the rate of change of phase. It can be seen from these tables that the mean and upper quartile of both the phase change and maximum rate of change of phase increase with increasing optical classification. On the other hand, this tendency is not shown clearly by either the maximum phase change or the maximum rate of change of phase. This is possibly because the change in height of the D region is related to the solar zenith angle [Chilton, et al., 1963].

3. Acknowledgments

The observations at College were made under the supervision of Dr. H. F. Bates at the Geophysical Institute, University of Alaska. Those at Frankfurt were made under the supervision of Dr. J. Eitzenberger of the Battelle Institute. The observations at Maui were made by Sada Katahara, while those at Boulder were under the supervision of A. H. Diede. The VLF program at Frankfurt, College, and Boulder is supported by the Advanced Research Projects Agency, Washington, D. C.

4. References

- Bracewell, R. N., and T. W. Straker (1949), The study of solar flares by means of very long radio waves, Monthly Notices, Roy. Ast. Soc. 109, 28.
- Chilton, C. J., F. K. Steele, and R. B. Norton (1963), VLF phase observations of solar flare ionization in the D region of the ionosphere, J. Geophys. Res. 68, 5421-5435.
- Wait, J. R. (Nov. 5, 1959), Diurnal change of ionospheric heights deduced from phase velocity measurements at VLF, Proc. IRE 47, 998.
- Wait, J. R. (1962), Comments on a paper by W. D. Westfall, Prediction of VLF diurnal phase changes and solar flare effect, J. Geophys. Res. 67, 916.

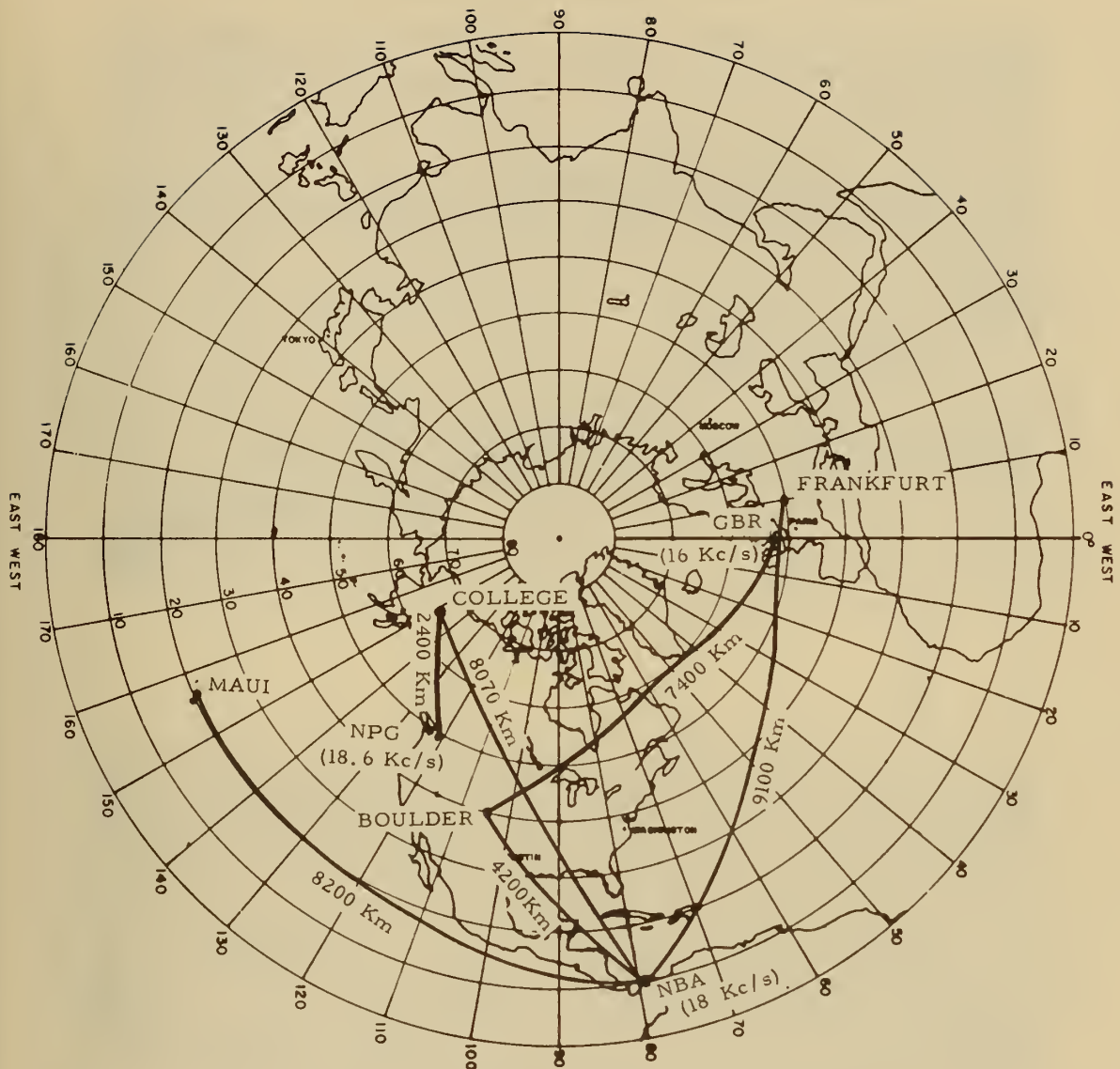
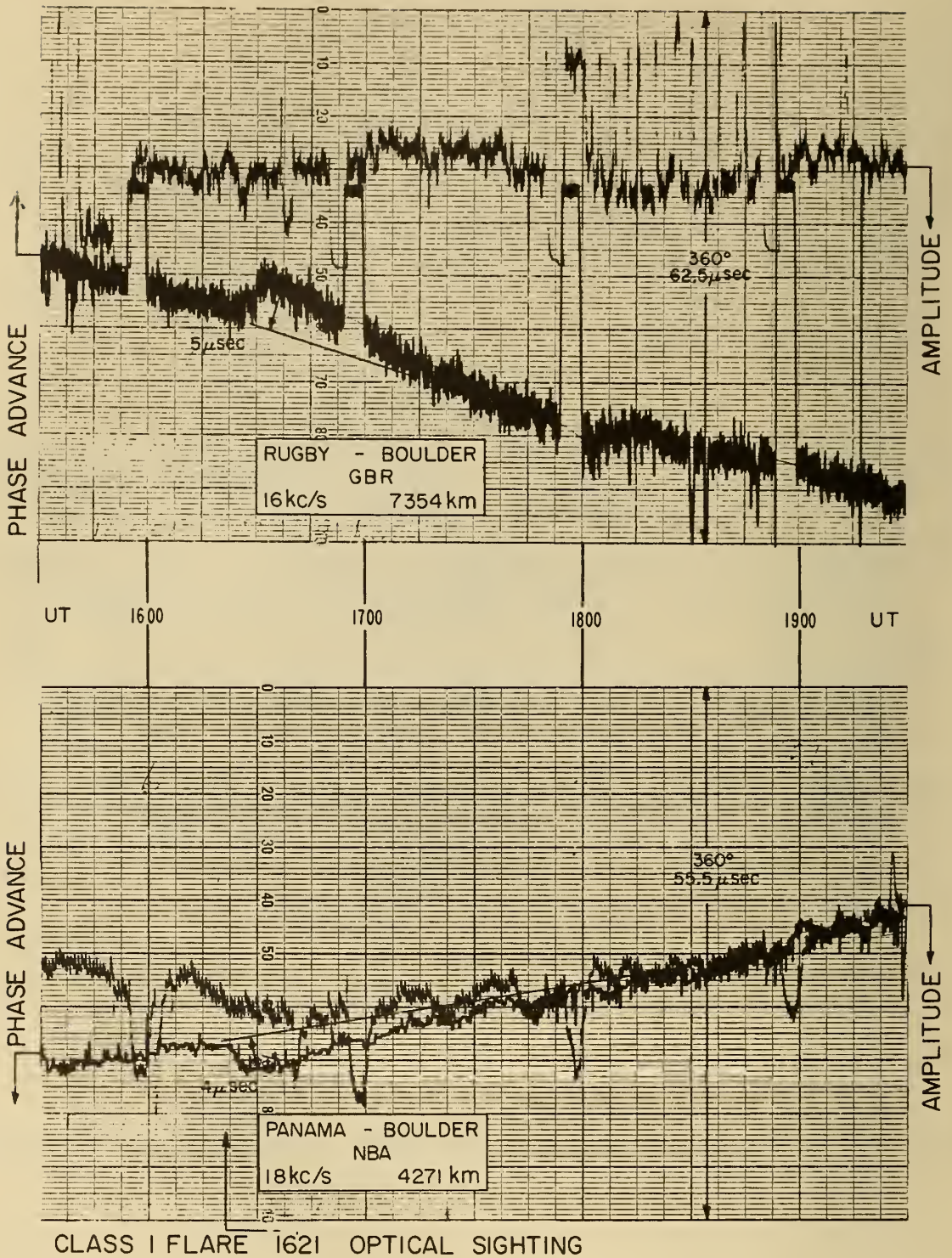


Figure 1. Map showing the paths and transmitter frequencies used in this Note.

SUDDEN PHASE ANOMALY 1 - MAY 1961 UT



CLASS I FLARE 1621 OPTICAL SIGHTING

Figure 2

SUDDEN PHASE ANOMALY 5-JUNE 1961 UT

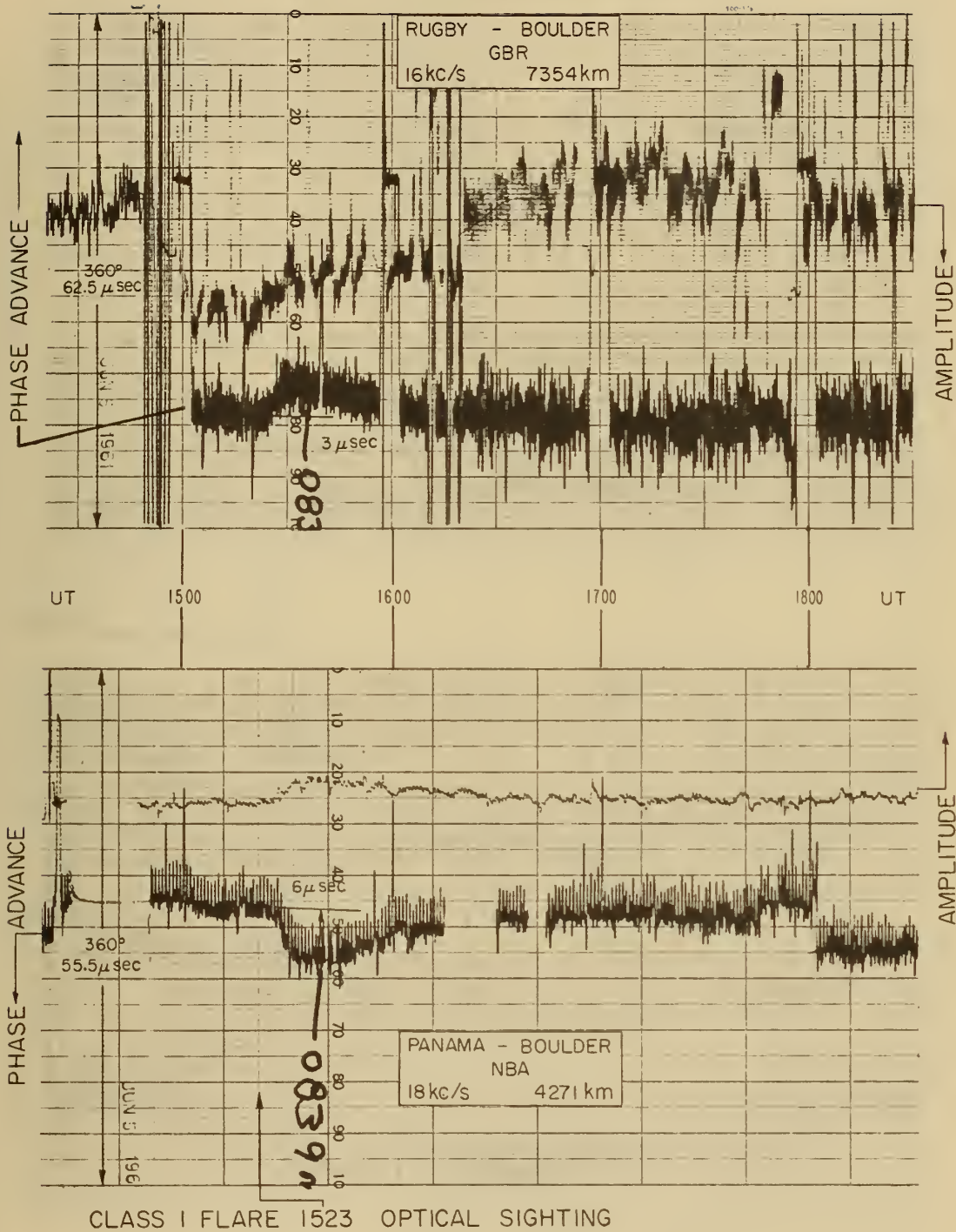


Figure 3

SUDDEN PHASE ANOMALY 11-JULY 1961 UT

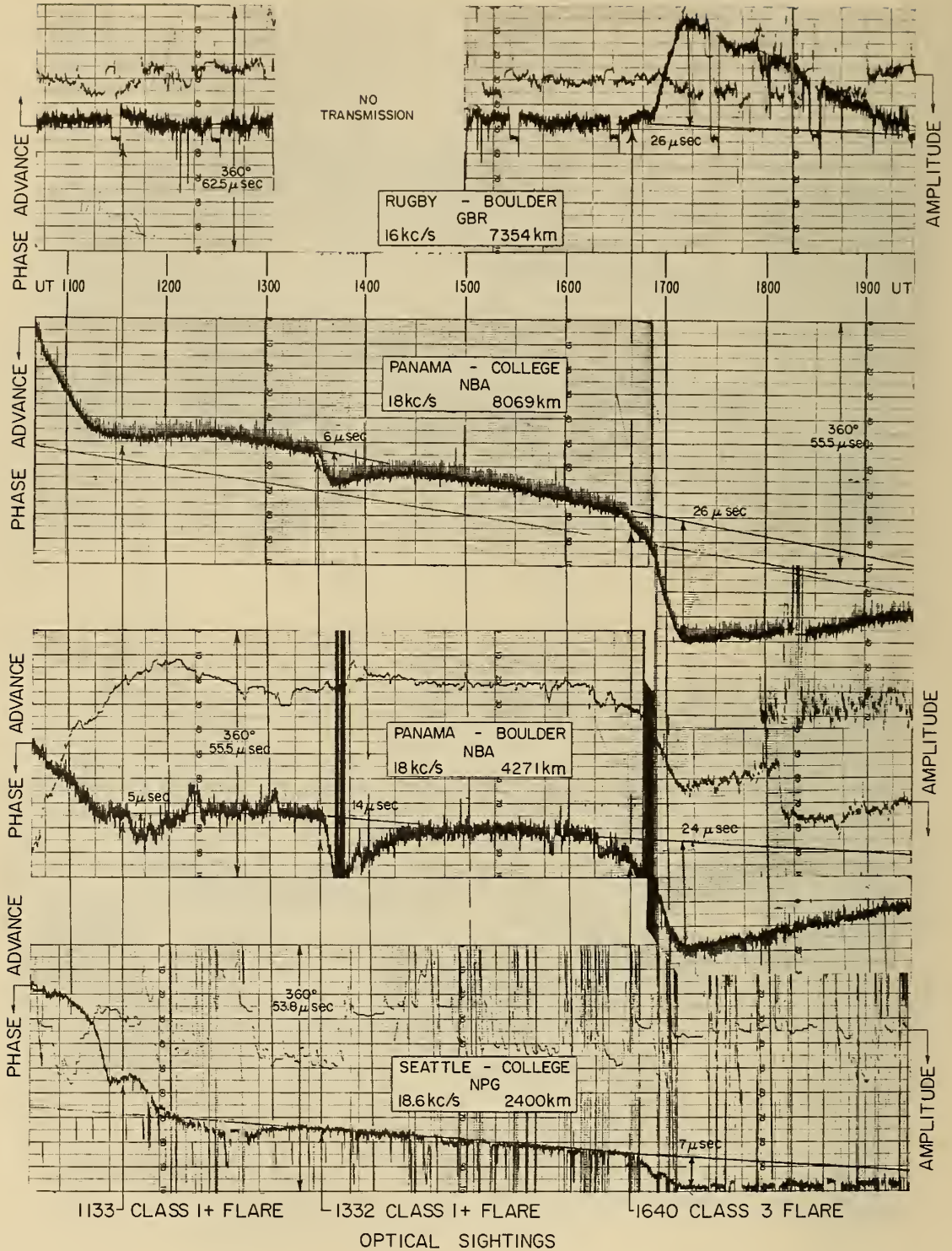


Figure 4

SUDDEN PHASE ANOMALY 15-JULY 1961 UT

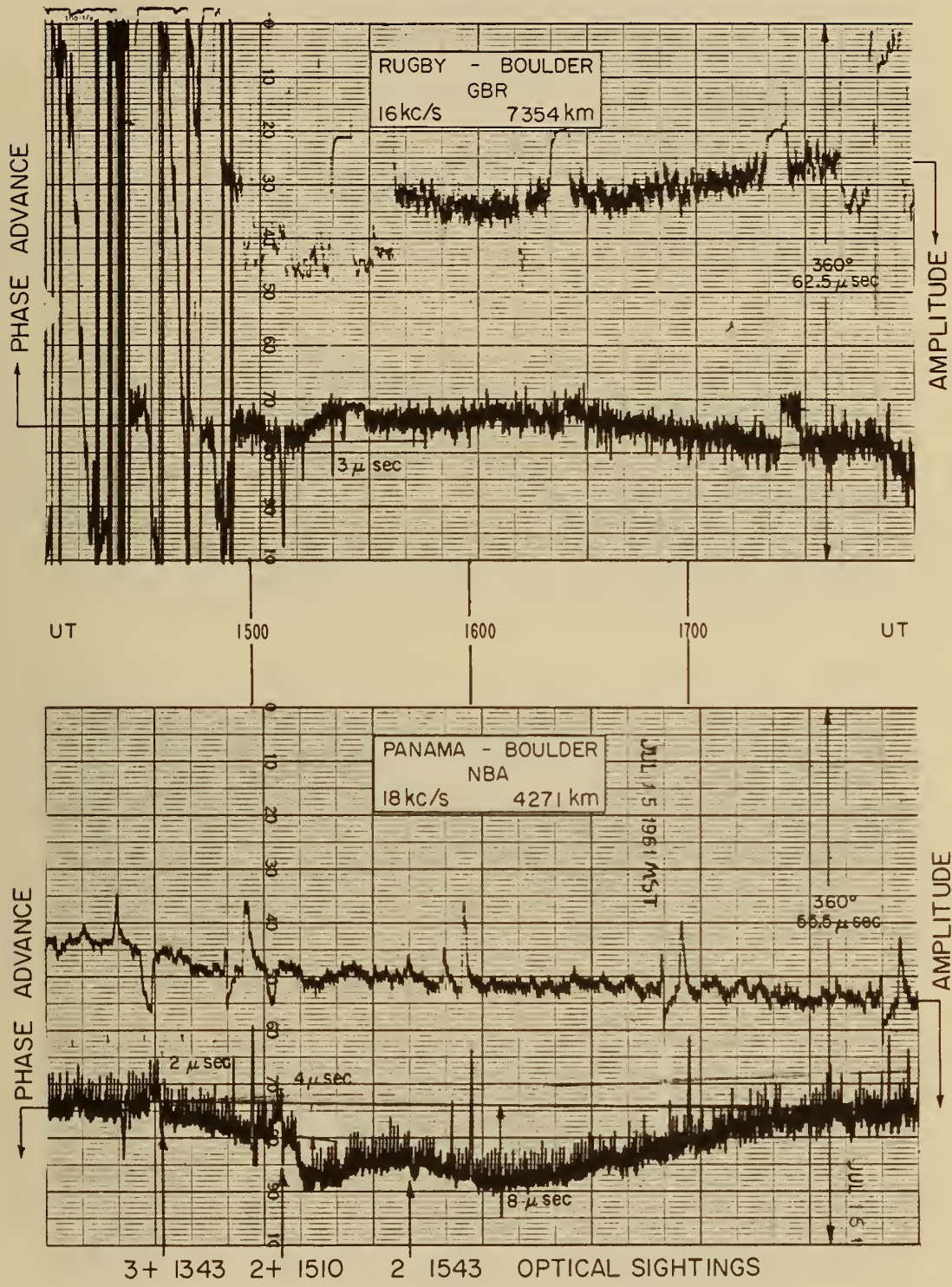


Figure 5

SUDDEN PHASE ANOMALY 17-JULY 1961 UT

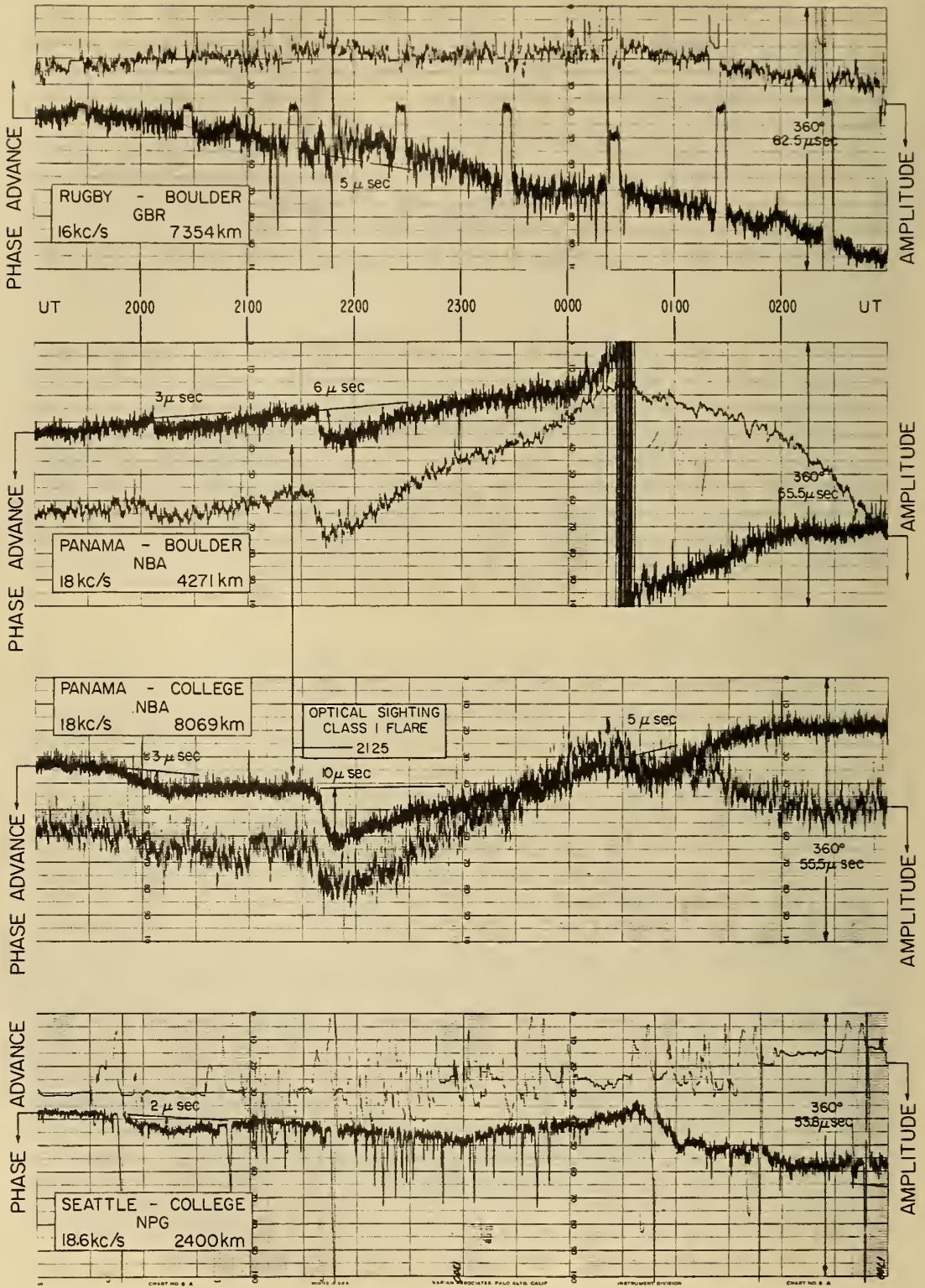


Figure 6

SUDDEN PHASE ANOMALY 18-JULY 1961 UT

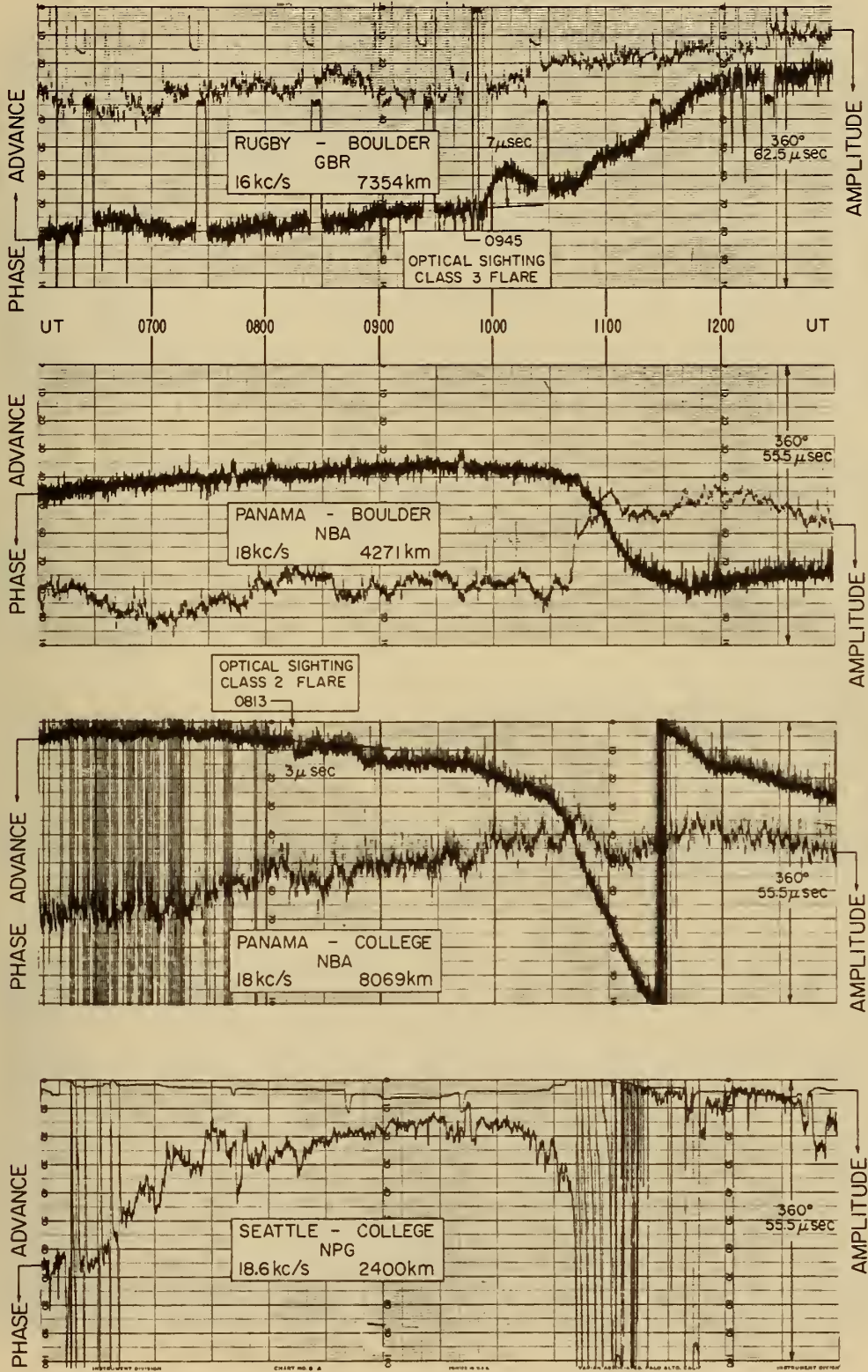


Figure 7

SUDDEN PHASE ANOMALY 20-JULY 1961 UT

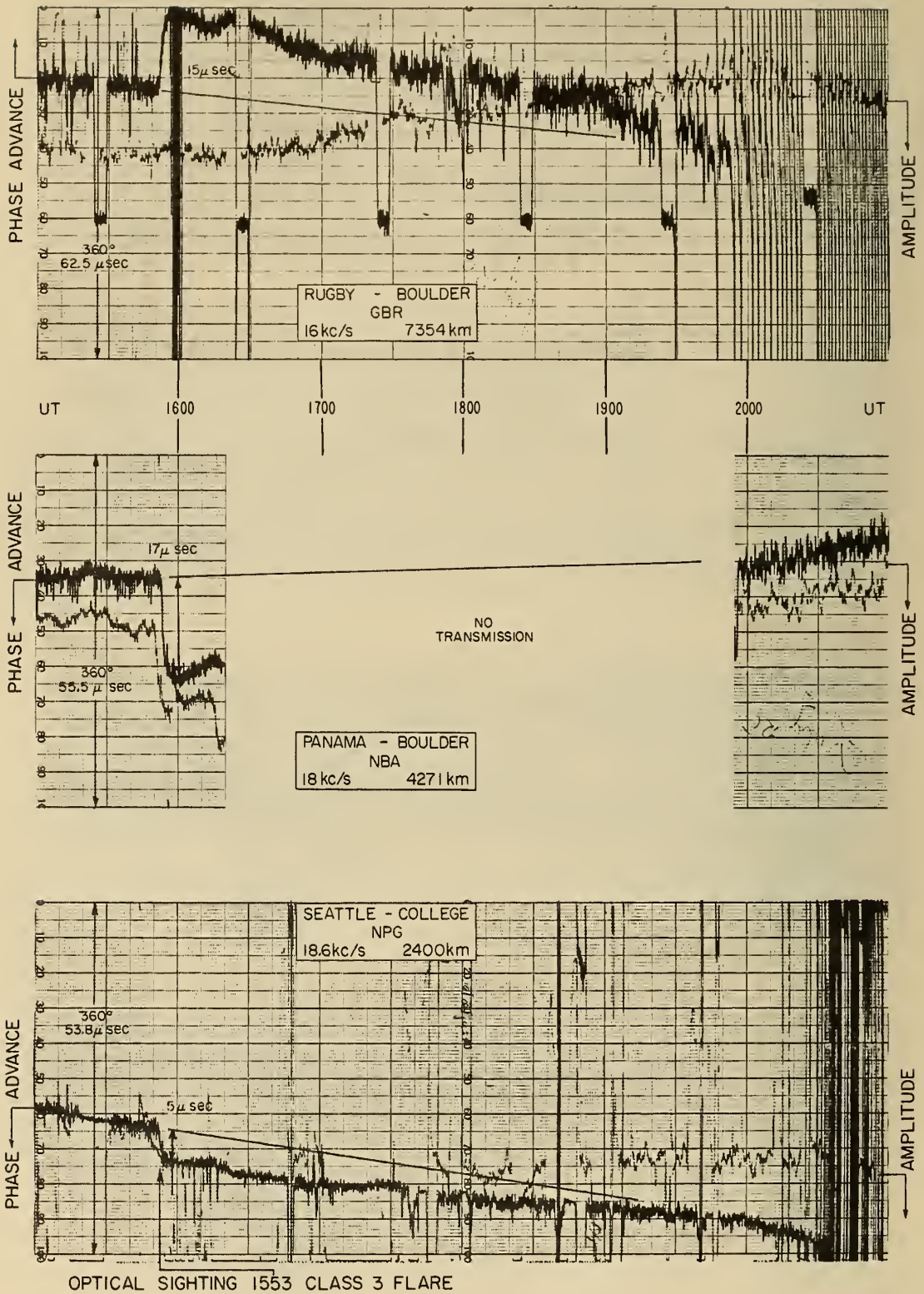


Figure 8

SUDDEN PHASE ANOMALY 21-JULY 1961 UT

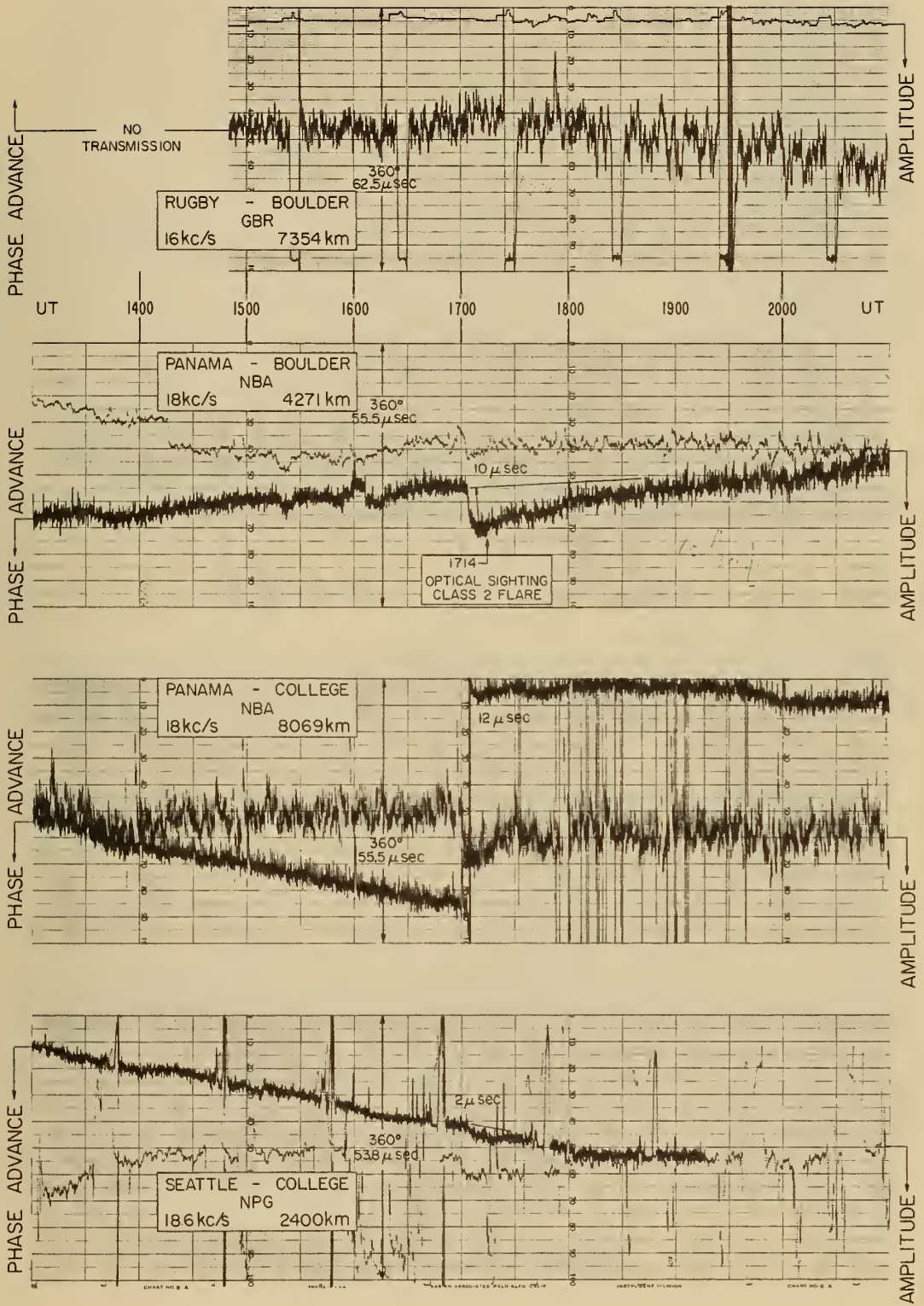
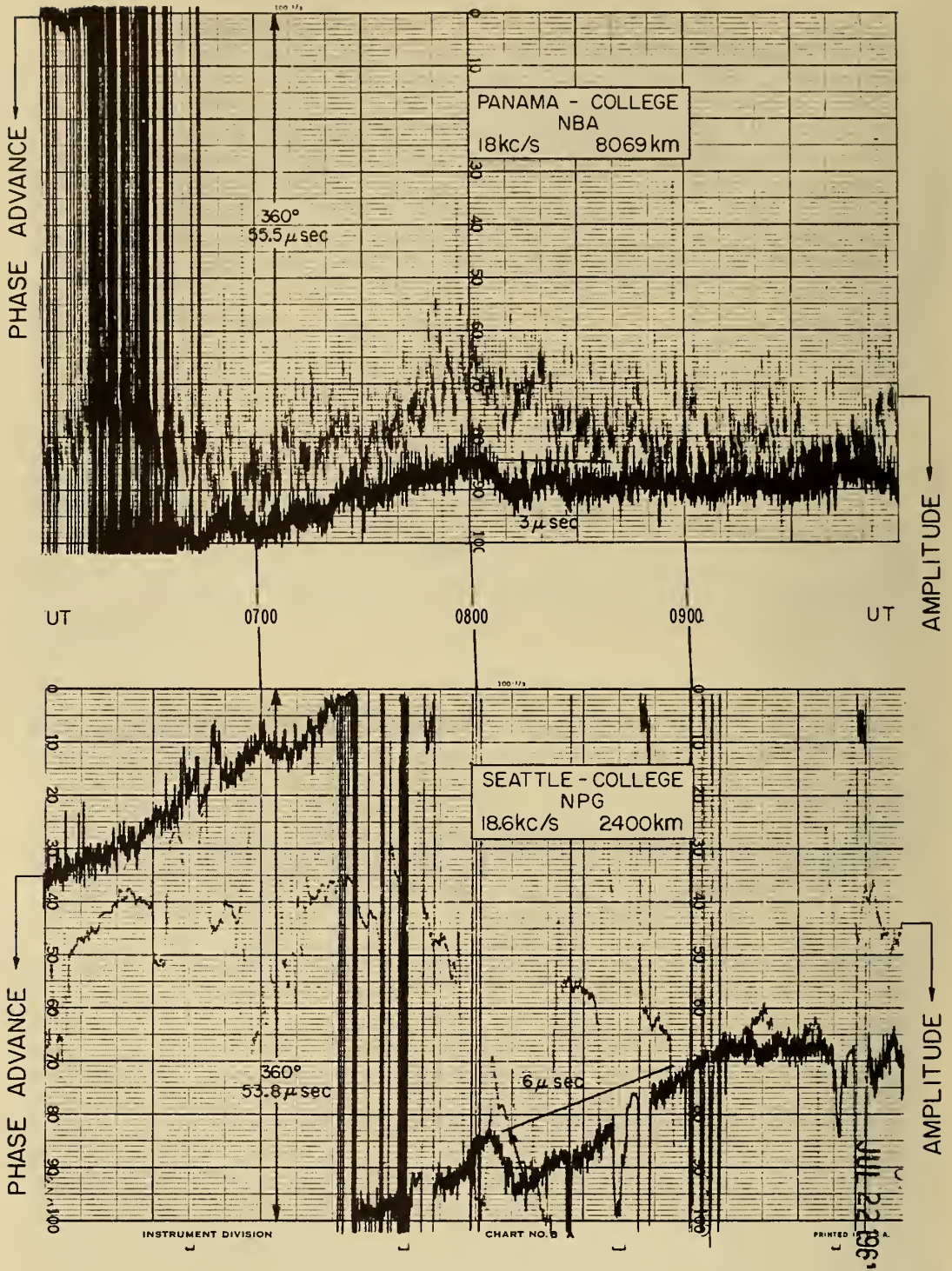


Figure 9

SUDDEN PHASE ANOMALY 23-JULY 1961 UT



NO OPTICAL SIGHTING

Figure 10

SUDDEN PHASE ANOMALY 24-JULY 1961 UT

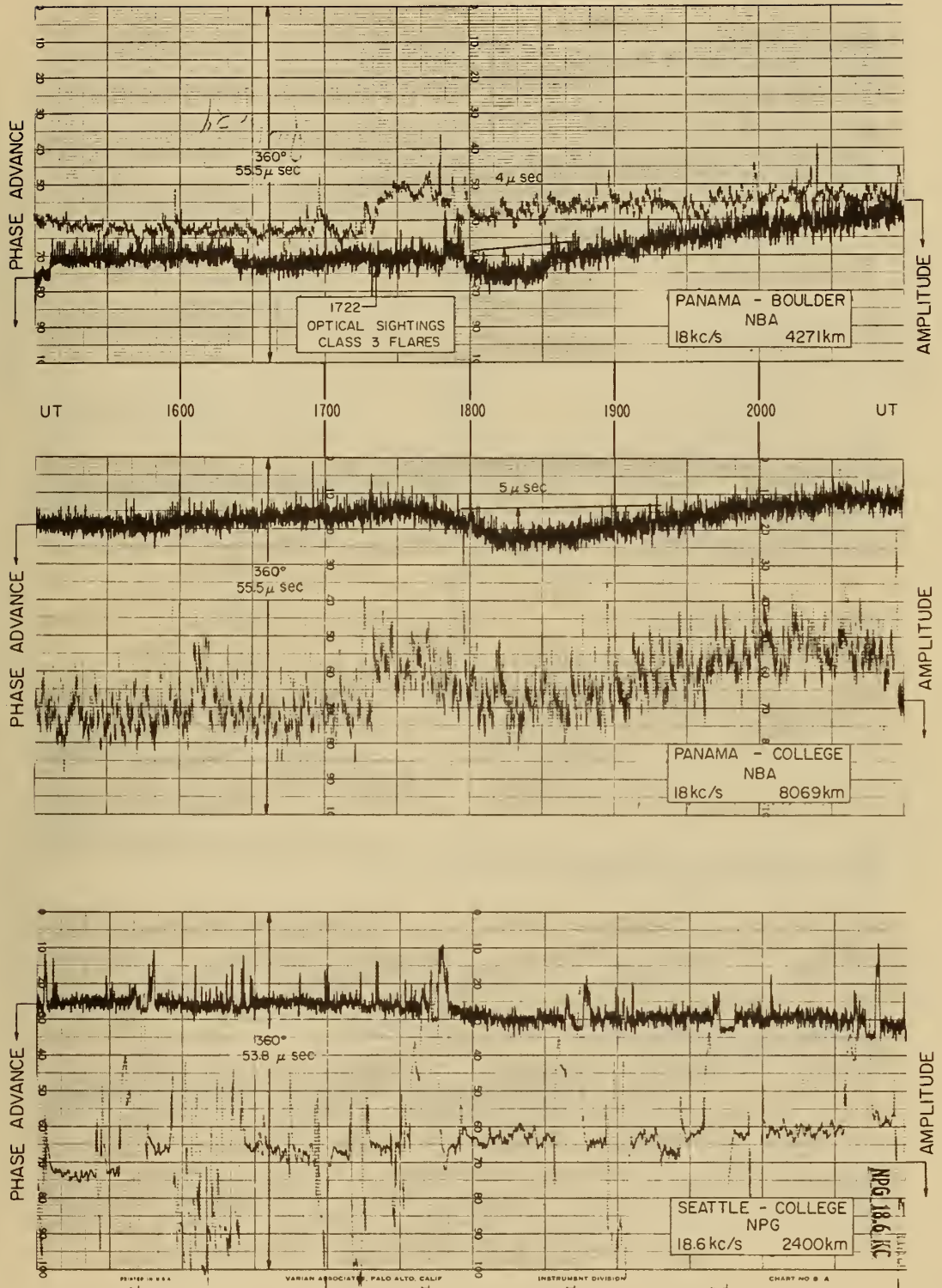


Figure 11

SUDDEN PHASE ANOMALY 15-AUGUST 1961 UT

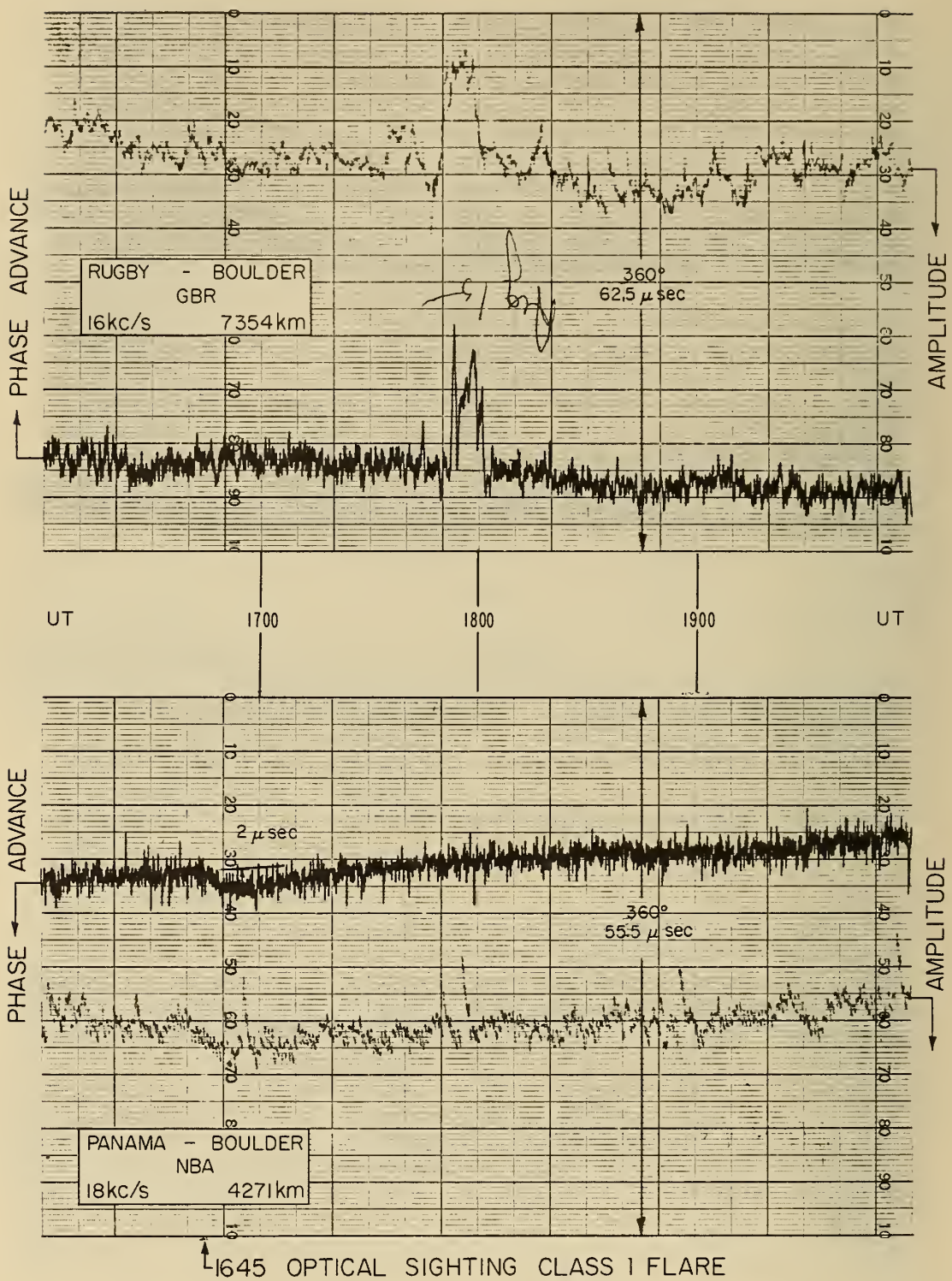


Figure 12

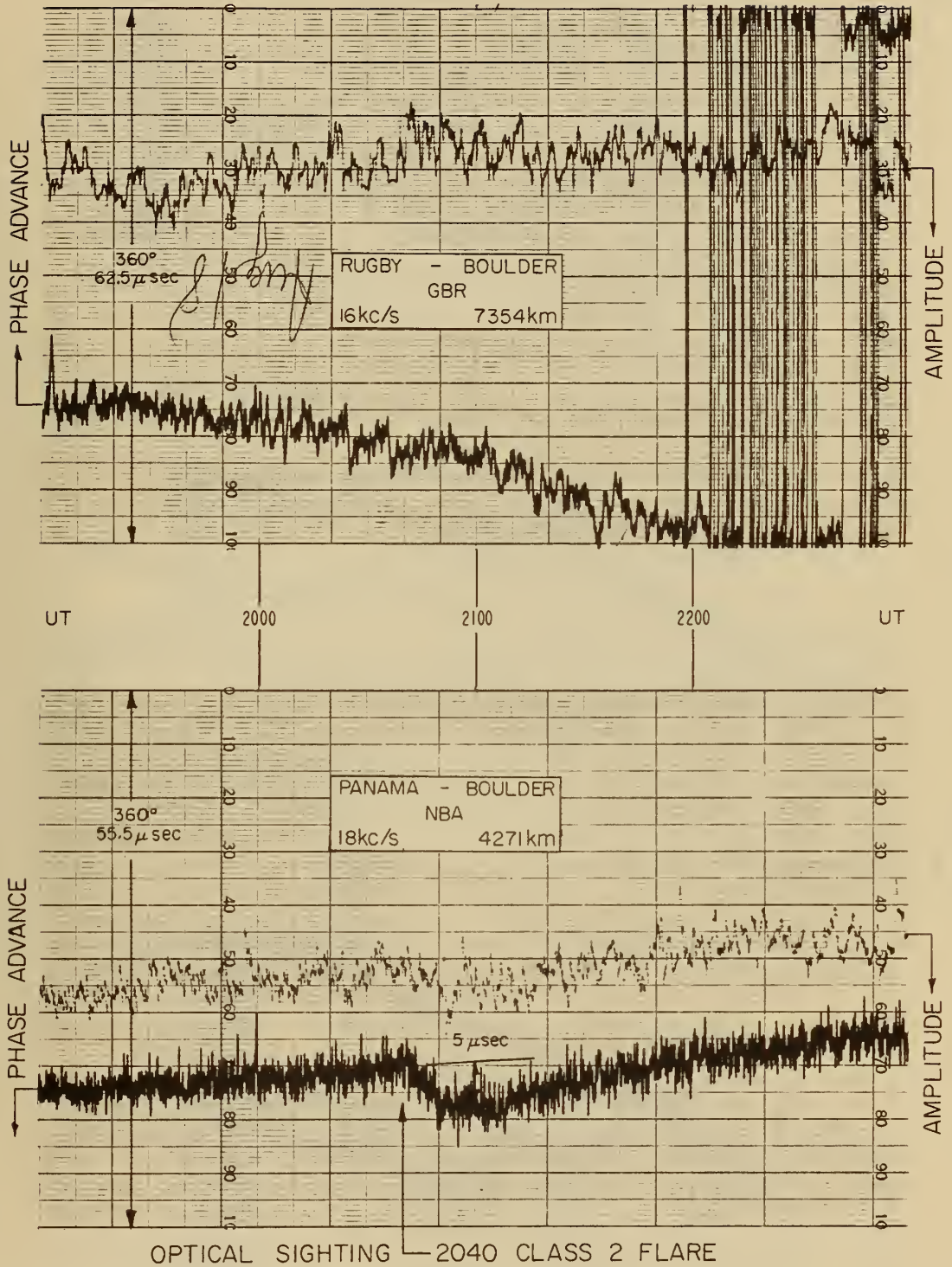


Figure 13

SUDDEN PHASE ANOMALY 1-SEPTEMBER 1961 UT

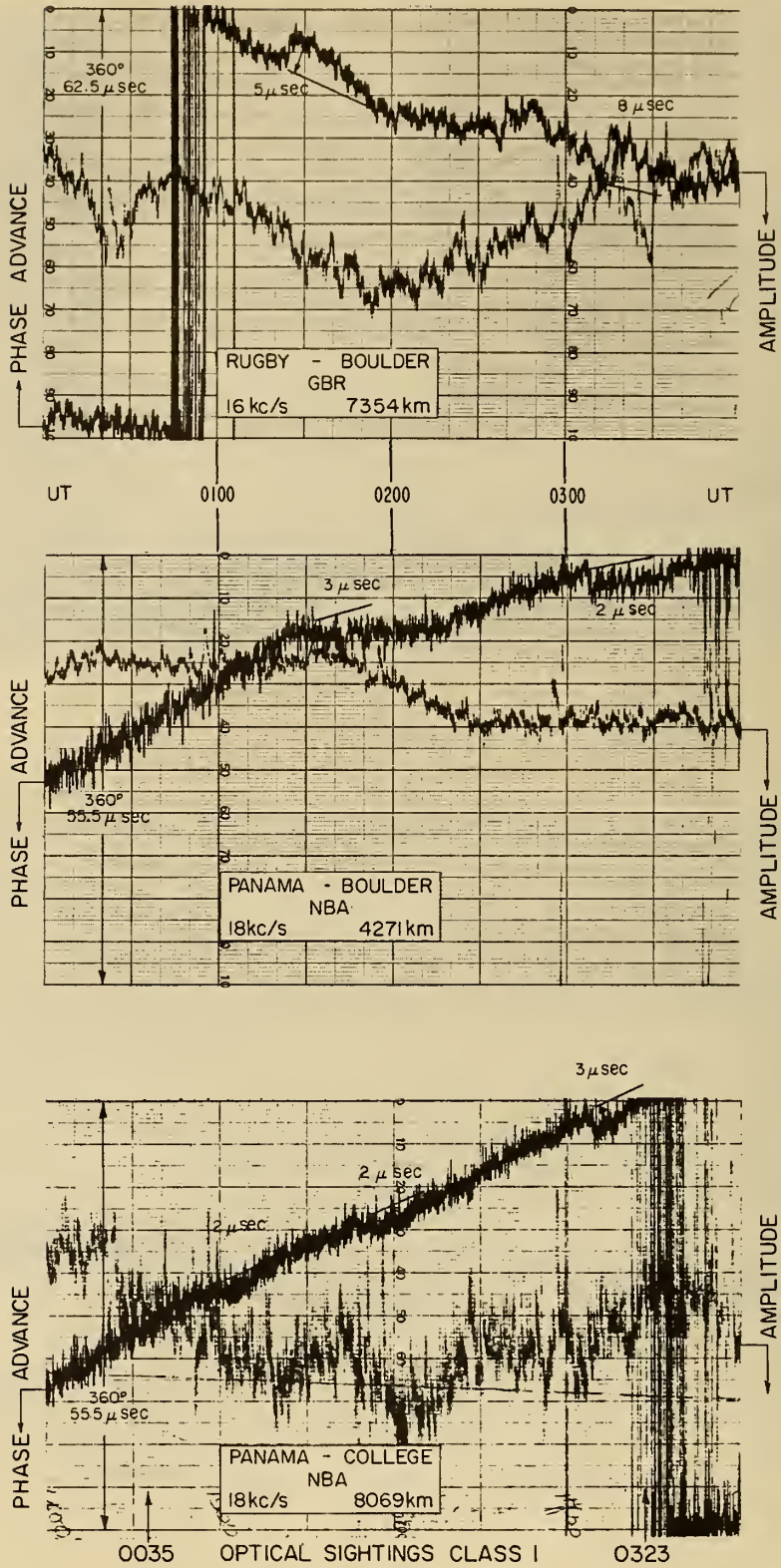


Figure 14

SUDDEN PHASE ANOMALYS 2-SEPTEMBER 1961 UT

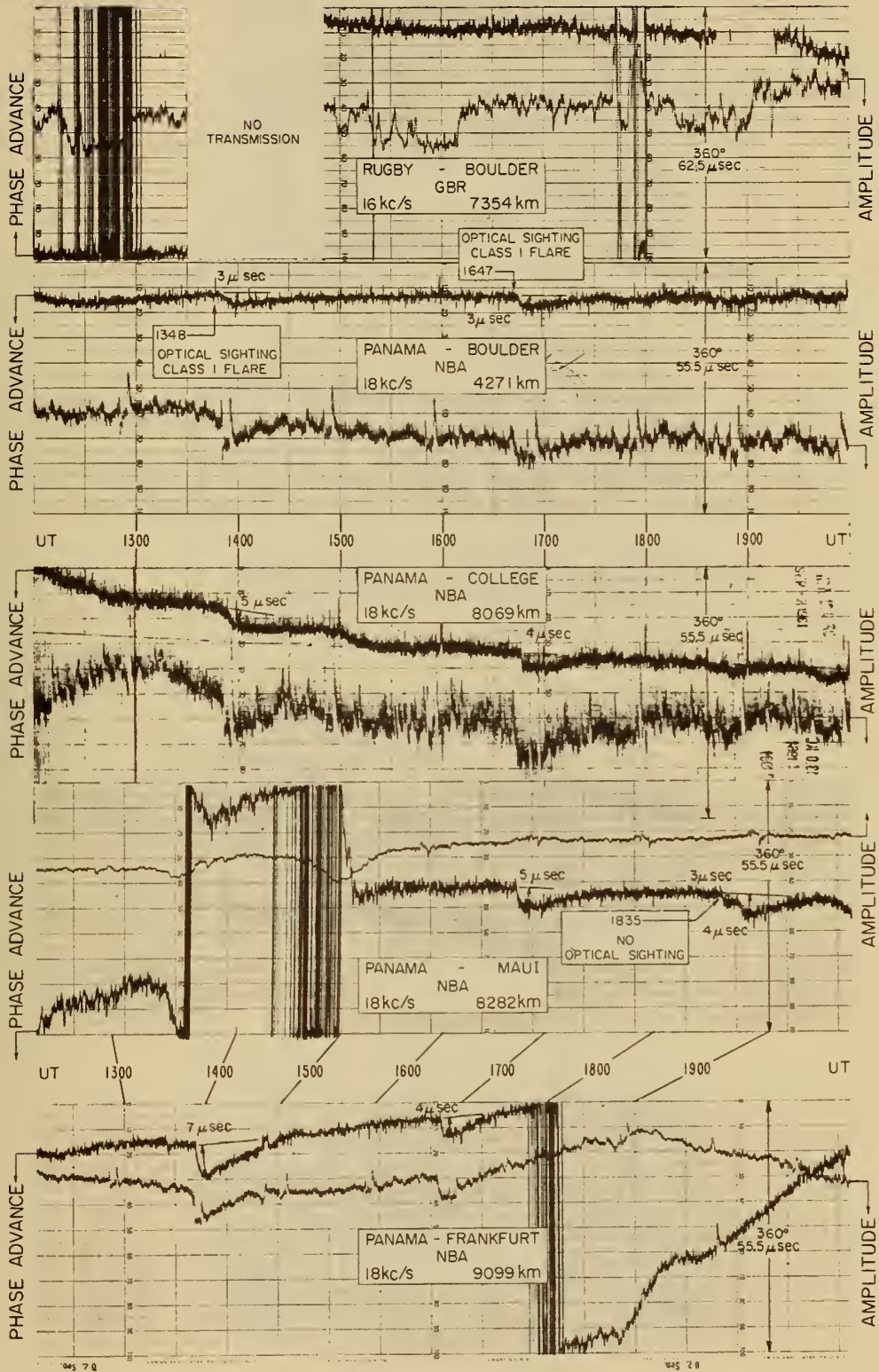


Figure 15

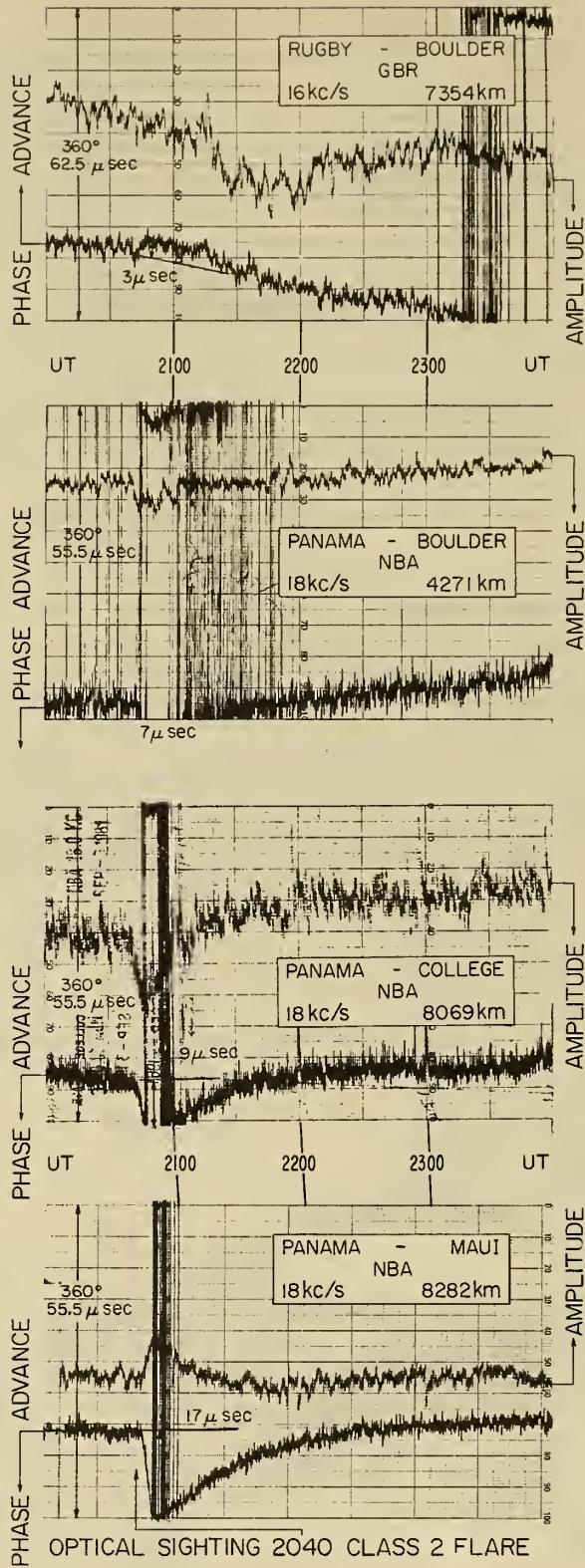


Figure 16

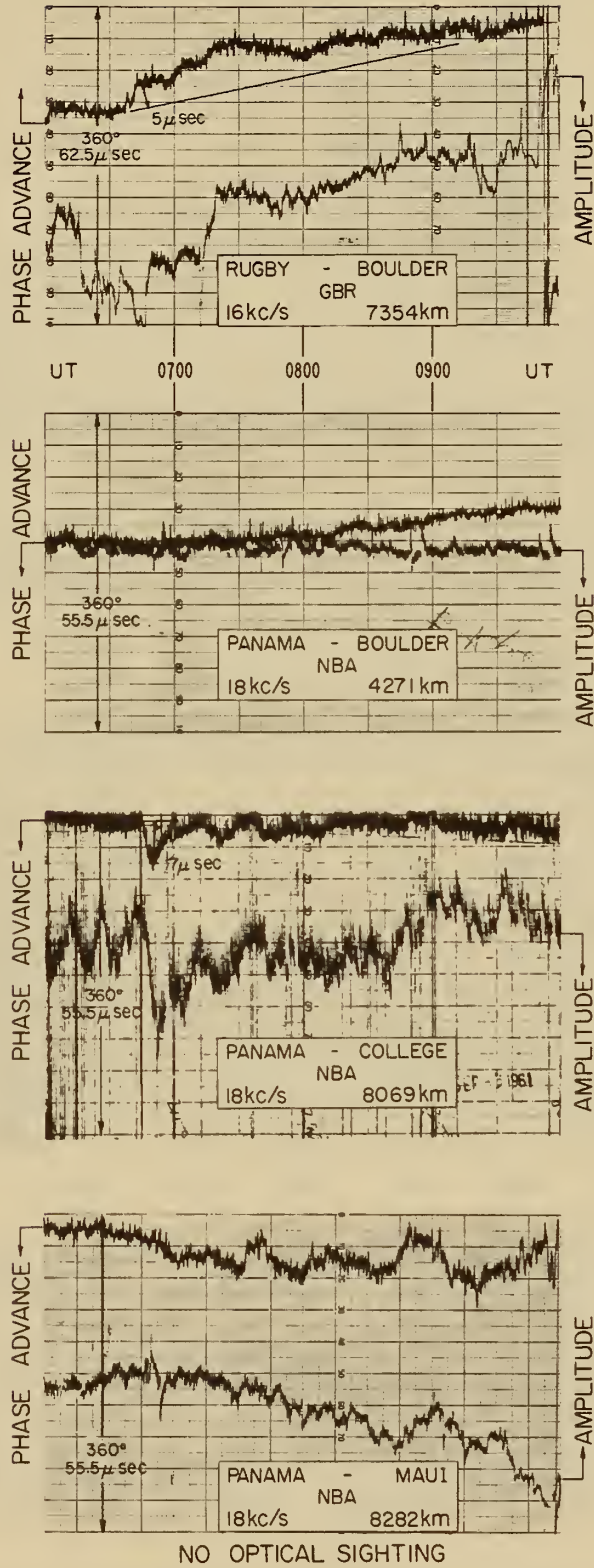
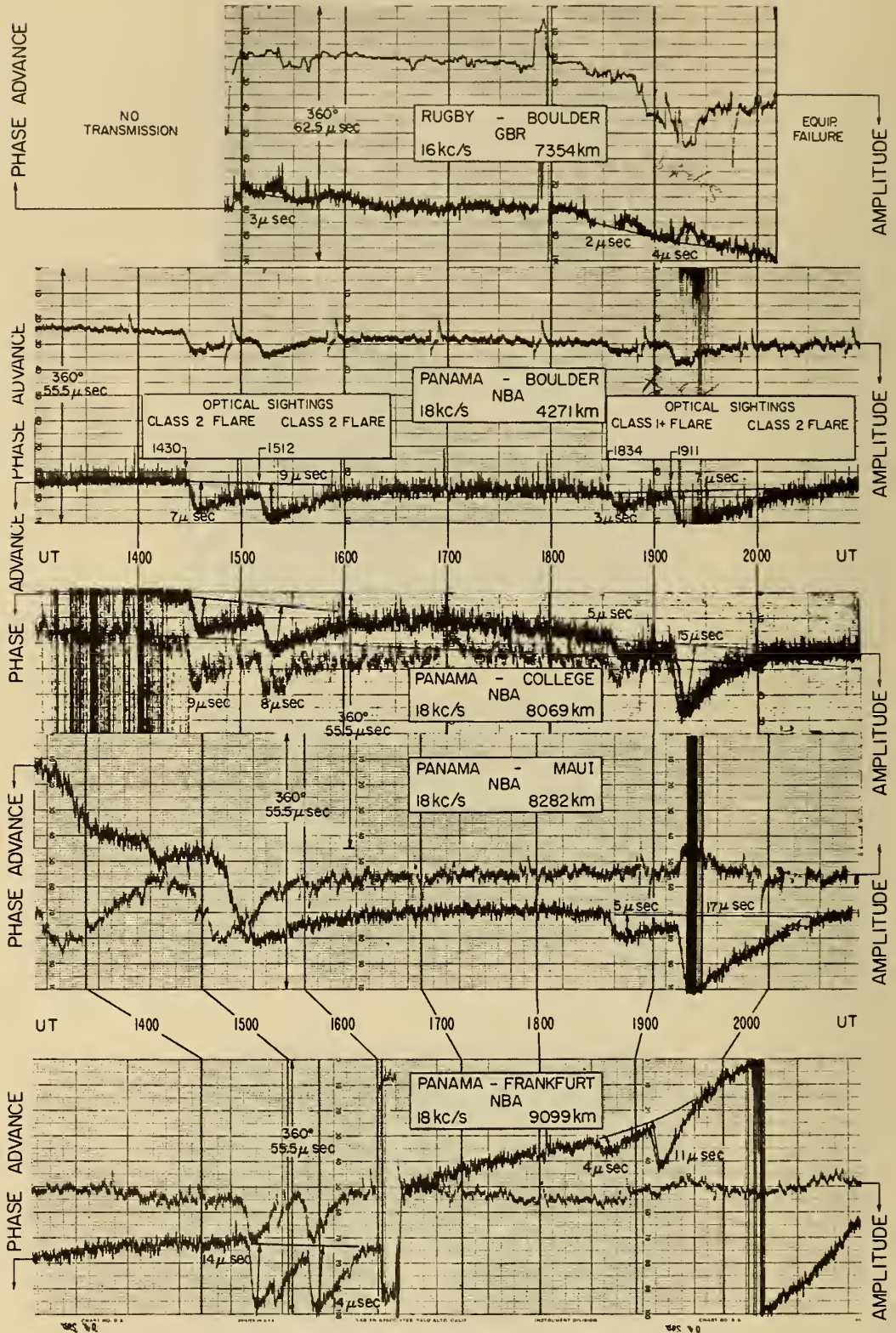


Figure 17a

SUDDEN PHASE ANOMALY 4-SEPTEMBER 1961 UT



Multiple path SPA observations of 4 solar flares which occurred on 4 September 1961 UT.

Figure 17b

SUDDEN PHASE ANOMALY 5-SEPTEMBER 1961 UT

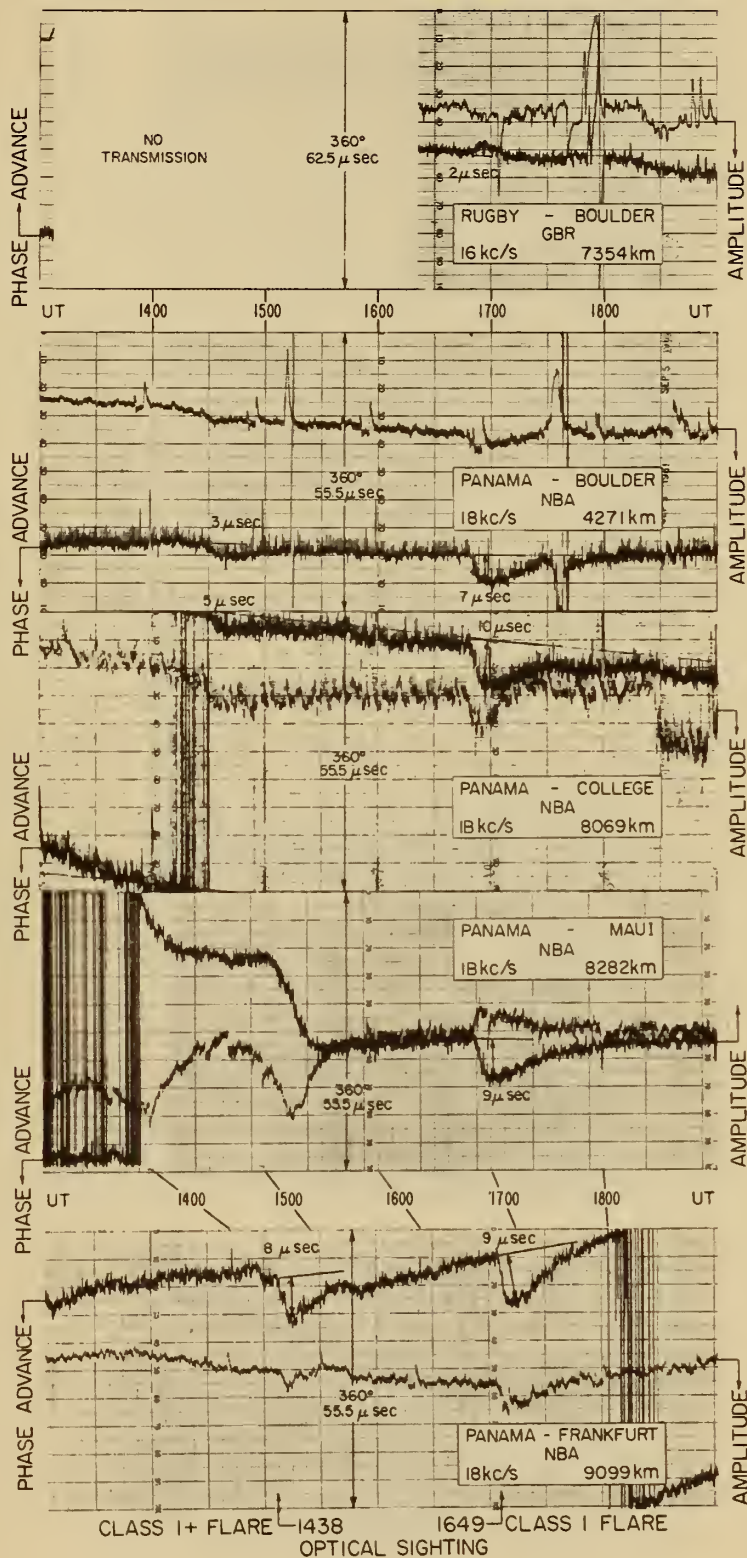


Figure 18

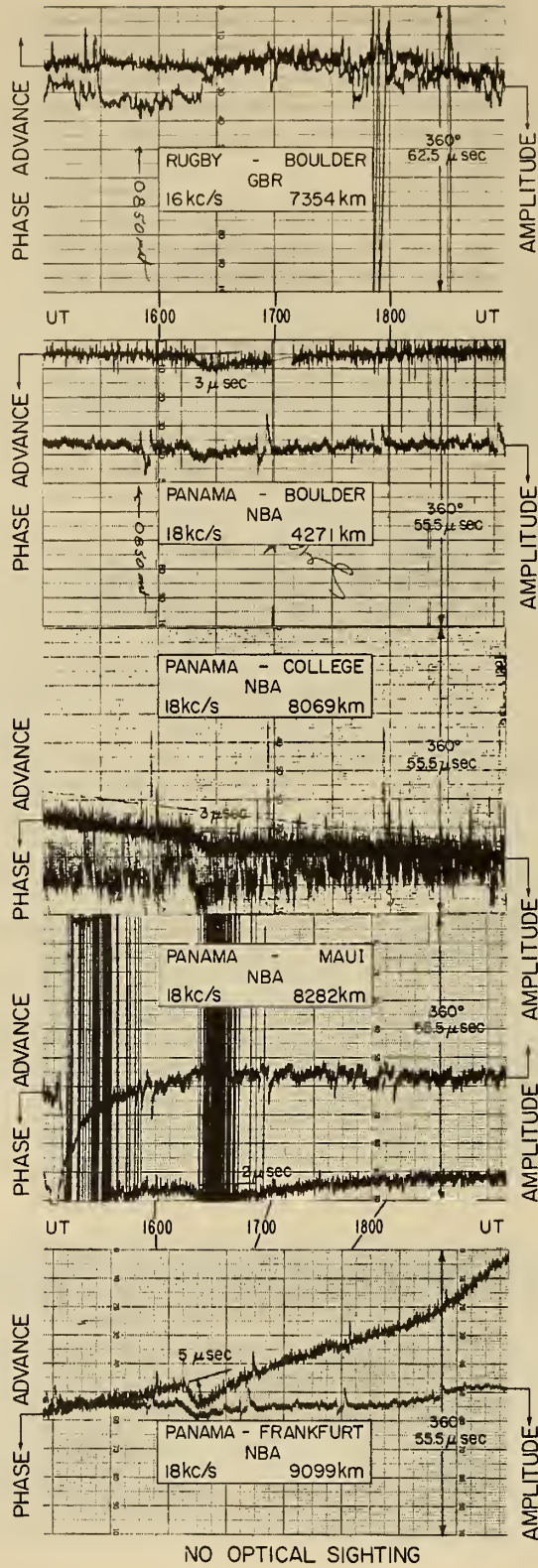


Figure 19

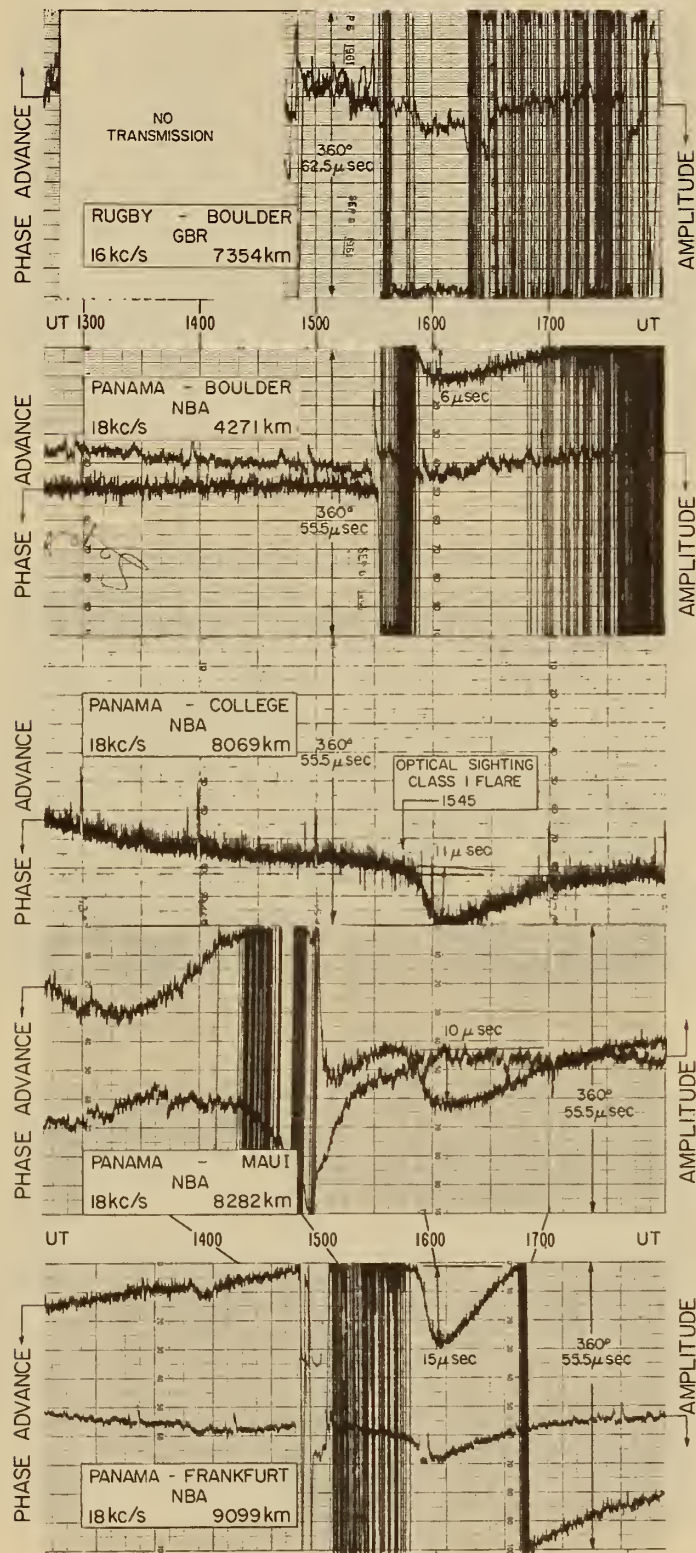


Figure 20

SUDDEN PHASE ANOMALY 5 - NOVEMBER 1961 UT

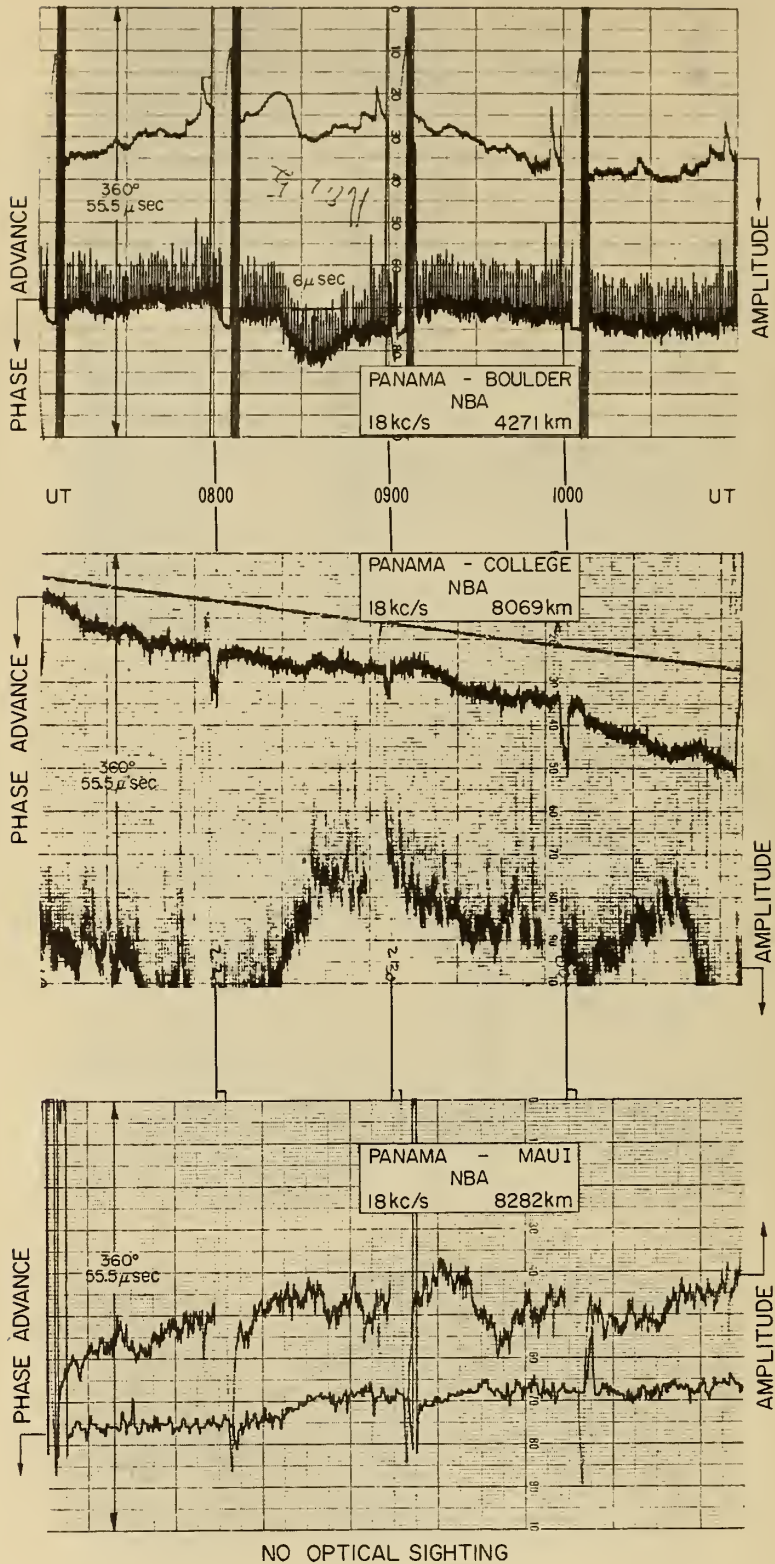


Figure 21

SUDDEN PHASE ANOMALY 10-NOVEMBER 1961 UT

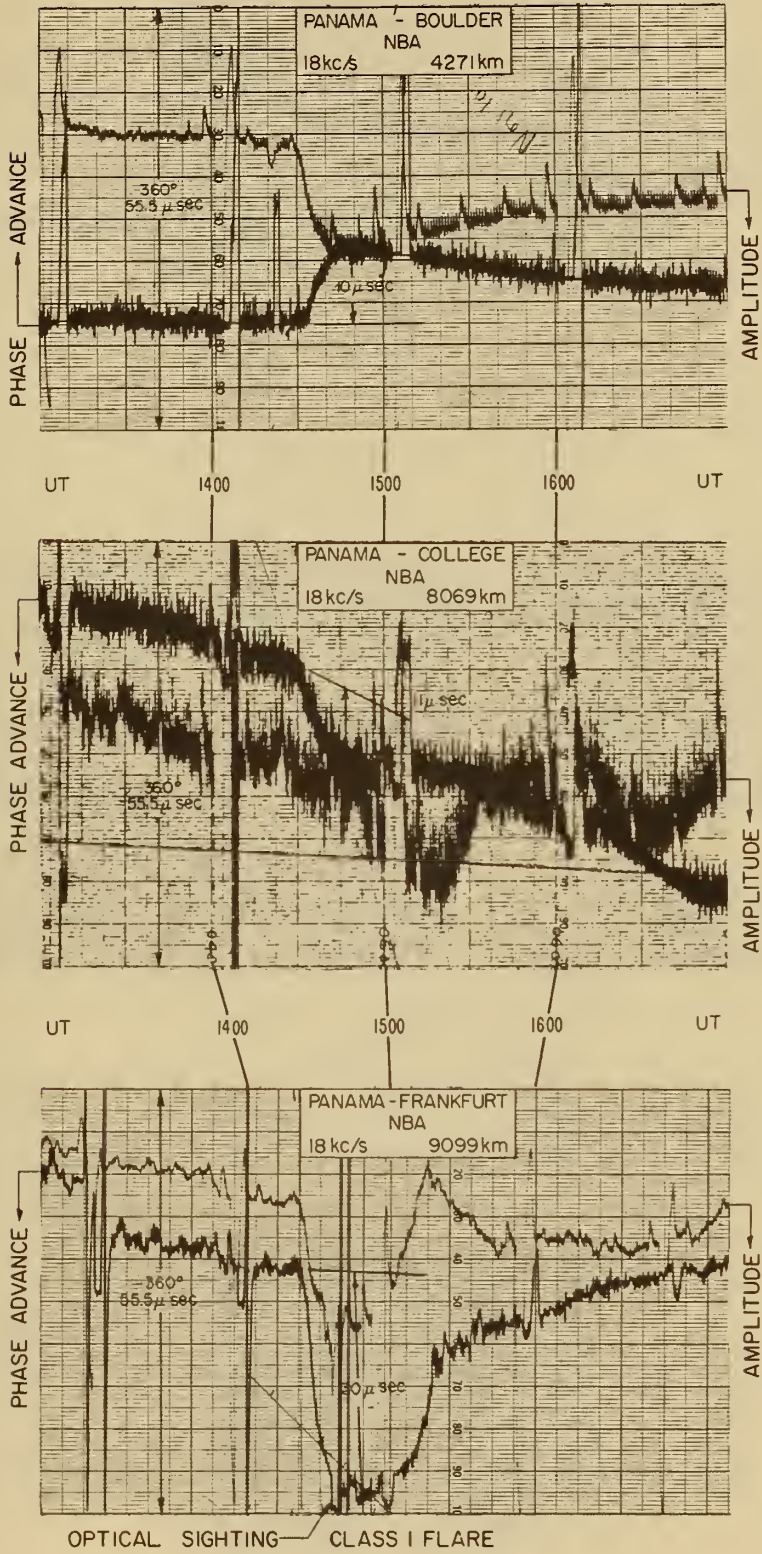


Figure 22

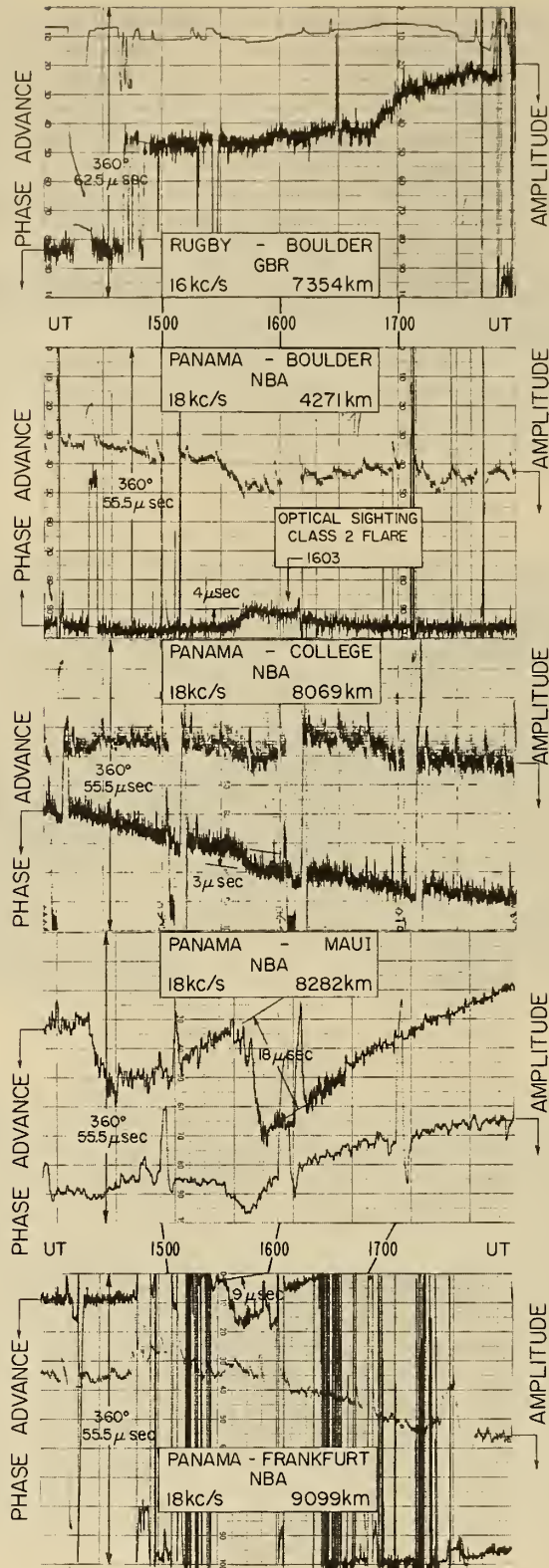


Figure 23

SUDDEN PHASE ANOMALY 2-DECEMBER 1961 UT

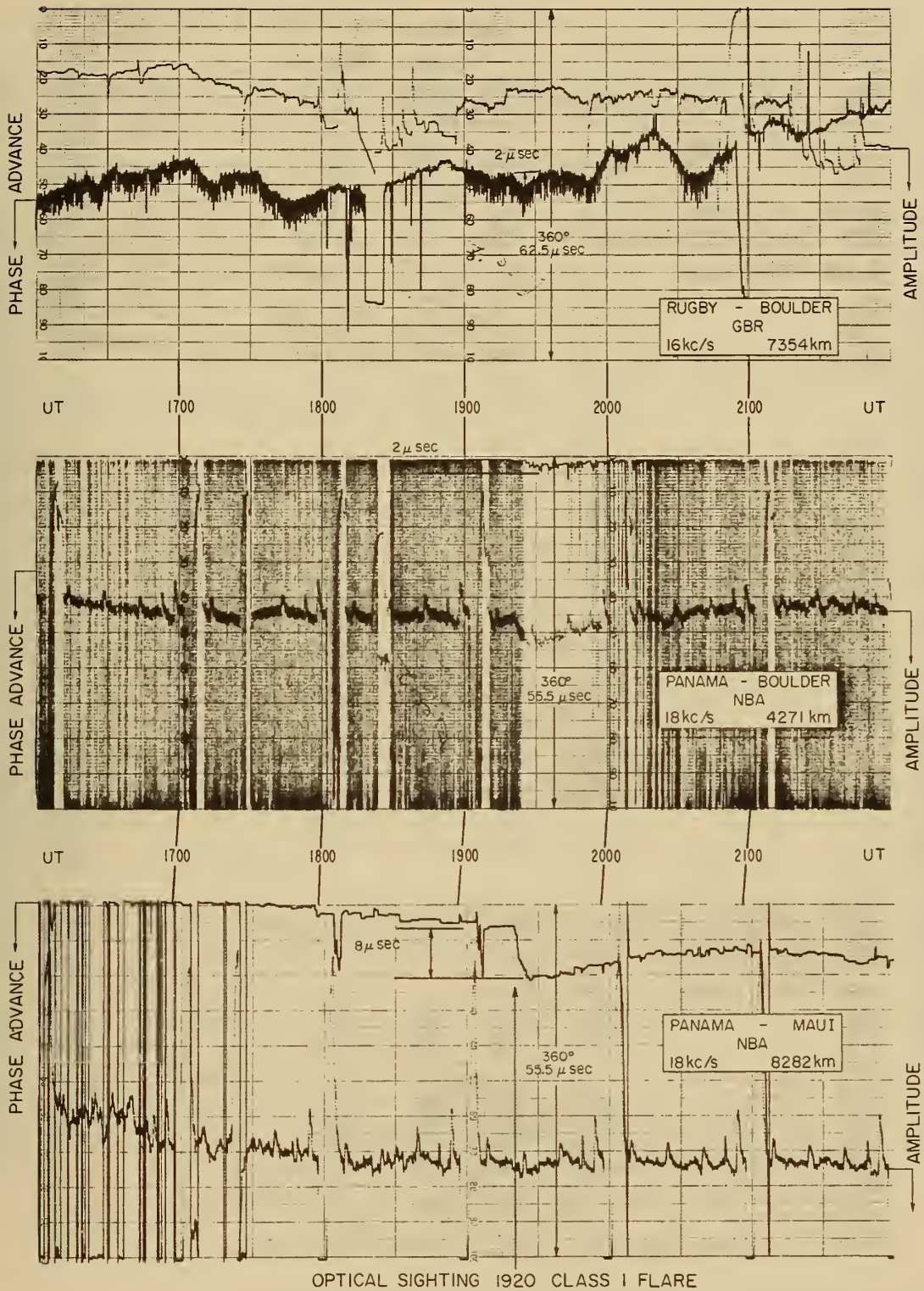


Figure 24

TABLE No. 1

Flare Number	Date 1961	Optical Class	Optical Sighting UT	Time of Beginning SPA (UT)	Time of Maximum SPA (UT)	End Time SPA (UT)	$\Delta \varphi$ Degrees	$\Delta \varphi$ Micro Sec	Δh Km	$\frac{d\varphi}{dt}$ Deg/Min	χ Ave. Degrees	Average Cos χ
1	1 May	1	1621									
NBA-BO				1623	1630	1852	26	4	2.2	4	27.51	.88689
GBR-BO				1623	1634	1745	29	5	1.4	3	47.35	.67747
2	5 Jun	1	1523									
NBA-BO				1523	1538	1644	39	6	3.3	4	38.23	.78550
GBR-BO				1523	1534	1650	17	3	0.8	2	41.58	.74801
3	11 Jul	1+	1133									
NBA-BO				1135	1142	1225	32	5	2.7	9	87.11	.05029
GBR-BO											61.22	.43133
NBA-CO											86.88	.05439
NPG-CO											90.00	.0000
4	11 Jul	1+	1332									
NBA-BO				1334	1340	1500	91	14	7.6	12	63.35	.44843
NBA-CO				1335	1340	1450	39	6	1.7	7	67.81	.37756
NPG-CO											82.00	.13913
5	11 Jul	3	1640									
GBR-BO				1636	1712	2000	150	26	8.6	8	41.36	.75050
NBA-CO				1634	1710	2100	168	26	8.5	10	38.27	.78501
NBA-BO				1616	1710	2000	155	24	15.0	7	24.41	.91058
NPG-CO				1633	1711	2100	47	7		1	58.48	.52268
6	15 Jul	2+	1510									
NBA-BO				1511	1517		26	4	2.2	9	42.44	.73791
GBR-BO				1510	1526		17	3	0.8	2	43.23	.72861
7	17 Jul	No Optical Sighting										
NBA-BO				2007	2015	2120	19	3	1.6	10	29.33	.87173
GBR-BO											57.92	.53104
NBA-CO				1951	2012	2100	19	3	0.9	1	34.05	.82847
NPG-CO				1950	2012	2112	13	2		2	37.98	.78815
8	17 Jul	1	2125									
NBA-BO				2140	2147	2330	39	6	3.3	40	49.20	.65335
GBR-BO				2140	2210	2342	29	5	1.4	1	63.67	.44352
NBA-CO				2140	2148	2348	65	10	2.8	14	46.77	.68492
NPG-CO											37.77	.79048
9	18 Jul	2	0813									
NBA-BO											90.00	.0000
GBR-BO											72.37	.30283
NBA-CO				0813	0815		19	3	0.9	13	90.00	.0000
NPG-CO											90.00	.0000
10	18 Jul	3	0945									
NBA-BO											90.00	.0000
GBR-BO				0956	1006	1035	40	7	2.0	4	66.10	.40498
NBA-CO											90.00	.0000
NPG-CO											90.00	.0000
11	20 Jul	3	1553									
GBR-BO				1553	1557	1950	86	15	5.0	30	42.70	.73491
NBA-BO				1553	1600	2000	110	17	10.6	90	34.18	.82724
NPG-CO				1553	1557	2000	33	5		30	65.74	.41078
12	21 Jul	2	1714									
GBR-BO											43.41	.72635
NBA-BO				1702	1710	2000	64	10	6.2	42	19.86	.94050
NBA-CO				1702	1710	2000	78	12	3.9	22	35.94	.80960
NPG-CO				1703	1712	1753	13	2		1	56.45	.55264

TABLE No. 1 (page 2)

Flare Number	Date 1961	Optical Class	Optical Sighting UT	Time of Beginning SPA (UT)	Time of Maximum SPA (UT)	End Time SPA (UT)	$\Delta \varphi$ Degrees	$\Delta \varphi$ Micro Sec	Δh Km	$\frac{d\varphi}{dt}$ Deg/Min	χ Ave. Degrees	Average Coa χ
13	23 Jul	No Optical Sighting										
NBA-CO				0803	0815	0842	19	3	0.9	3	90.00	0000
NPG-CO				0804	0813	0900	40	6		5	90.00	0000
14	24 Jul	3	1722									
NBA-BO				1750	1815	1930	26	4	2.2	1	13.44	.97261
NBA-CO				1730	1820	1950	32	5	1.4	1	31.80	.84985
NPG-CO											51.06	.62845
15	15 Aug	1	1645									
NBA-BO				1645	1655	1750	13	2	1.1	2	25.12	.90540
GBR-BO											48.65	.66053
16	18 Aug	2	2040									
NBA-BO				2040	2100	2210	32	5	2.7	2	39.36	.77316
GBR-BO											62.90	.45542
17	1 Sep	No Optical Sighting										
NBA-BO				0130	0140		19	3	1.6	1	89.35	.01133
GBR-BO				0125	0130	0200	29	5	1.4	3	89.17	.01441
NBA-CO											78.23	.20384
18	1 Sep	No Optical Sighting										
NBA-BO											90.00	0000
GBR-BO											90.00	0000
NBA-CO				0150	0200	0230	13	2	0.6	2	78.84	.19343
19	1 Sep	1	0323									
NBA-BO				0307	0318	0352	52	8	4.3	1	90.00	0000
GBR-BO				0310	0312	0350	12	2	0.6	10	90.00	0000
NBA-CO				0308	0315	0346	19	3	0.9	2	83.41	.11463
20	2 Sep	1	1348									
NBA-BO				1350	1400	1500	19	3	1.6	2	65.79	.40943
GBR-BO											60.65	.49006
NBA-CO				1350	1400	1500	32	5	1.4	3	71.00	.32544
NBA-MA											72.02	.30855
NBA-FK				1351	1400	1500	45	7	1.8	23	42.42	.73817
21	2 Sep	1	1647									
NBA-BO				1646	1651	1730	19	3	1.6	2	28.12	.88191
GBR-BO											54.22	.58454
NBA-CO				1646	1651	1730	26	4	1.2	14	45.91	.69573
NBA-MA				1645	1651	1735	32	5	1.4	14	49.79	.64553
NBA-FK				1646	1652	1731	26	4	1.0	11	42.95	.73187
22	2 Sep	No Optical Sighting										
NBA-BO											21.86	.92806
GBR-BO											60.08	.49878
NBA-CO											39.15	.77545
NBA-MA				1835	1837		19	3	0.8	1	30.06	.86544
NBA-FK											55.49	.56649
23	2 Sep	No Optical Sighting										
NBA-BO											22.52	.92369
GBR-BO											60.74	.48875
NBA-CO											39.17	.77527
NBA-MA				1843	1850	1927	26	4	1.1	8	28.98	.87473
NBA-FK											56.39	.55347
24	3 Sep	2	2040									
GBR-BO				2043	2050	2130	17	3	1.0	5	65.01	.42240
NBA-BO				2043	2051	2130	45	7	4.3	4	43.16	.72943
NBA-CO				2041	2050	2242	58	9	3.3	14	48.18	.66672
NBA-MA				2043	2051	2227	110	17	5.4	21	27.68	.88548

TABLE No. 1 (page 3)

Flare Number	Date 1961	Optical Class	Optical Sighting UT	Time of Beginning SPA (UT)	Time of Maximum SPA (UT)	End Time SPA (UT)	$\Delta \phi$ Degrees	$\Delta \phi$ Micro Sec	Δh Km	$\frac{d\phi}{dt}$ Deg/Min	χ Ave. Degrees	Average Cos χ
25	4 Sep	No Optical Sighting										
NBA-BO											90.00	0000
GBR-BO				0637	0645		29	5	1.4	9	84.52	.09538
NBA-CO				0645	0650		45	7	2.0	13	90.00	0000
NBA-MA											90.00	0000
26	4 Sep	2	1430									
NBA-BO				1429	1437		45	7	3.8	10	54.59	.57940
NBA-CO				1431	1436		58	9	2.6	24	64.55	.42972
NBA-MA											66.06	.40576
NBA-FK				1430	1438		91	14	3.6	23	38.98	.77731
27	4 Sep	2	1512									
NBA-BO				1510	1518	1650	58	9	4.9	16	45.88	.69612
GBR-BO				1510	1518	1532	17	3	0.9	2	55.54	.56575
NBA-CO				1512	1520	1641	52	8	2.3	10	58.97	.51538
NBA-MA											61.72	.47364
NBA-FK				1514	1520	1615	91	14	3.6	25	38.12	.78661
28	4 Sep	1	1834									
GBR-BO				1833	1843	1900	11	2	1.0	1	61.01	.48463
NBA-BO				1831	1841		19	3	1.8	5	22.73	.92233
NBA-CO				1837	1844		32	5	1.6	5	39.75	.76878
NBA-MA				1837	1846		32	5	1.9	27	29.84	.86740
NBA-FK				1836	1845		25	4	1.1	3	56.08	.55803
29	4 Sep	2	1911									
GBR-BO				1910	1919	1940	23	4	1.3	4	61.60	.47560
NBA-BO				1910	1917	2045	45	7	3.0	10	26.85	.89219
NBA-CO				1912	1919	2020	97	15	4.6	18	40.56	.75964
NBA-MA				1913	1921	2027	110	17	5.4	18	25.96	.89908
NBA-FK				1910	1917	1943	71	11	2.4	12	59.32	.51016
30	5 Sep	1+	1438									
NBA-BO				1430	1440	1510	19	3	1.6	2	54.68	.57807
NBA-CO				1430	1440	1520	32	5	1.4	3	64.38	.43239
NBA-MA											66.07	.40548
NBA-FK				1439	1446	1520	52	8	2.0	6	39.25	.77432
31	5 Sep	1	1649									
NBA-BO				1650	1657	1800	45	7	3.8	7	27.64	.88582
GBR-BO				1650	1657	1710	12	2	0.6	2	55.43	.56734
NBA-CO				1650	1656	1825	65	10	2.9	10	45.88	.69614
NBA-MA				1651	1702	1823	58	9	2.5	10	48.49	.66263
NBA-FK				1649	1700	1810	58	9	2.3	14	44.58	.71225
32	7 Sep	No Optical Sighting										
GBR-BO											55.57	.56542
NBA-BO				1618	1628	1730	19	3	1.8	2	33.39	.83491
NBA-CO				1618	1628	1730	19	3	0.9	2	50.17	.64038
NBA-MA				1620	1632	1722	13	2	0.6	1	55.39	.56795
NBA-FK				1620	1626	1729	32	5	1.4	4	41.97	.74347
33	8 Sep	1	1545									
GBR-BO											55.96	.55973
NBA-BO				1531	1603	1730	39	6	4.3	6	38.53	.78227
NBA-CO				1551	1605	1723	71	11	3.6	6	53.99	.58789
NBA-MA				1547	1611	1745	65	10	3.2	8	57.88	.53155
NBA-FK				1542	1602	1742	97	15	4.4	12	40.44	.76102
34	5 Nov	No Optical Sighting										
NBA-BO				0822	0833	0920	39	6	3.3	4	90.00	0000
NBA-CO											90.00	0000
NBA-MA											90.00	0000

TABLE No. 1 (page 4)

<u>Flare Number</u>	<u>Date 1961</u>	<u>Optical Class</u>	<u>Optical Sighting UT</u>	<u>Time of Beginning SPA (UT)</u>	<u>Time of Maximum SPA (UT)</u>	<u>End Time SPA (UT)</u>	$\Delta \phi$ <u>Degrees</u>	$\Delta \phi$ <u>Micro Sec</u>	Δh <u>Km</u>	$\frac{d\phi}{dt}$ <u>Deg/Min</u>	χ Ave. <u>Degrees</u>	Average <u>Cos χ</u>
35	10 Nov	1	1434									
NBA-BO				1434	1449	1700	65	10	6.2	8	65.05	.42169
NBA-CO				1434	1446	1543	71	11	3.6	7	68.35	.36878
NBA-FK				1423	1438	1700	194	30	9.3	28	58.62	.52059
36	16 Nov	2	1603									
NBA-BO				1533	1550	1650	26	4	2.2	3	55.39	.56793
GBR-BO											78.65	.19674
NBA-CO				1537	1550	1632	19	3	0.9	3	63.47	.44663
NBA-MA				1538	1552	1640	117	18	5.0	22	63.35	.44849
NBA-FK				1536	1549	1638	58	9	2.3	8	60.21	.49670
37	2 Dec	1	1920									
GBR-BO				1921	1926	1933	11	2	0.6	4	75.92	.24320
NBA-BO				1923	1932	1950	19	3	1.8	1	52.85	.60377
NBA-MA				1924	1930	1956	52	8	2.5	26	45.49	.70094

Table 2

Distribution of maximum phase shift $\Delta\phi$, with optical flare classification

Optical flare classification	1	2	3
maximum $\Delta\phi$ (in degrees)	30	18	28
mean $\Delta\phi$ (in degrees)	7	8	14
minimum $\Delta\phi$ (in degrees)	2	2	4
Value of $\Delta\phi$ exceeded 25% of time	9°	12°	24°
Value of $\Delta\phi$ exceeded 50% of time	5°	7°	7°
Value of $\Delta\phi$ exceeded 75% of time	3°	3°	5°

Table 3

Distribution of maximum rates of change of phase ($d\phi/dt$) with optical flare classification

Optical flare classification	1	2	3	
maximum $d\phi/dt$	40	42	90	degrees/min.
mean $d\phi/dt$	9	13	18	degrees/min.
minimum $d\phi/dt$	1	1	1	degrees/min.
Values of $d\phi/dt$ exceeded 25% of time	10	21	30	degrees/min.
Values of $d\phi/dt$ exceeded 50% of time	6	10	7	degrees/min.
Values of $d\phi/dt$ exceeded 75% of time	2	4	1	degrees/min.



